CRITICAL PROPERTIES

OF NaCl-H_2O SOLUTIONS.

by

Cheryl L. Erickson Knight

Thesis submitted to the Faculty of

Virginia Polytechnic Institute & State University

in partial fulfillment of the requirements of the degree of

MASTER OF SCIENCE

in

Geology

APPROVED:

Robert J. Bodnar, Chairman

J. Donald Rimstidt

Robert J. Tracy

January,1988

Blacksburg, Virginia

CRITICAL PROPERTIES OF NaCl-H_2O SOLUTIONS

by
Cheryl L. Erickson Knight

Committee Chairman: Robert J. Bodnar
Geological Sciences
(ABSTRACT)

Critical properties of the NaCl-H_2O fluid system are of fundamental interest to a variety of geochemical applications including fluid inclusion studies, numerical modeling of hydrothermal systems, and development of theoretical models for two-component fluid systems. Although many workers have expressed interest in NaCl-H_2O fluid critical properties, most studies have been limited to small compositional ranges with little agreement among data sets at higher salinities. Critical densities are recorded in only one of these reports, and no studies have determined the locations of NaCl-H_2O critical isochores (PT projections of critical densities). Furthermore, no studies to date have determined critical properties of NaCl-H_2O solutions in excess of room temperature saturation (26.4 wt.% NaCl).

Using the synthetic fluid inclusion technique, critical properties have been determined for NaCl-H_2O compositions from 0.0 to 30.0 wt.% NaCl. Critical temperatures and pressures range from 374°C and 220 bars for pure H_2O to 665°C and 930 bars for 25 wt.% NaCl. Critical temperatures for 27.5 and 30.0 wt.% NaCl are greater than 725°C. Critical densities and isochores were calculated using the equation of Bodnar (1985) relating molar volumes of NaCl-H_2O solutions to PTX properties above 1000 bars and below 1000°C. Critical densities for compositions from 0.0 to 25 wt.% NaCl range

from 0.3220 to 0.6440 g/cc, those of 27.5 and 30.0 wt.% NaCl are less than 0.6782 and 0.7092 g/cc, respectively. Empirical equations have been fit to plots of critical temperature, pressure and density in order to provide estimations of critical properties for compositions intemediate to those examined.

ACKNOWLEDGMENTS

I would like to extend a heartfelt thank you to my advisor, Bob Bodnar for everything; for turning me loose in his lab, providing direction, editing, financial and moral support for this project, and for the opportunity to work with his students. I wish to gratefully acknowledge the improvements made on this manuscript by and . I would like to nominate my "other advisor" for sainthood; for his patience in teaching me nearly everything I know about the practical aspects of experimental geochemistry, for being there with the answers when I needed them most. I am very thankful for the mental stimulation and moral support provided by , , , , , , , and most especially by my dear friend and role model, . I owe a debt of thanks, and a bottle of super glue, to , , , , , and , a.k.a. the "Brew'ry Boys", for instilling the fourth floor offices with a sense of hiliarity and fun (and for returning my desk). I would like to express my deep appreciation and admiration for my friend and first advisor, at the University of Iowa for being my inspiration. And , as always, for believing.

TABLE OF CONTENTS

LIST OF FIGURES

LIST OF TABLES

LIST OF EQUATIONS

INTRODUCTION

Fluids play an important role in a wide range of geologic processes, including diagenesis, metamorphism, volcanic eruptions, ore genesis, and even the preservation of fossils. Many of these processes occur at pressures and temperatures in the vicinity of fluid critical points and critical isochores, where relatively large fluctuations in density occur over small variations in temperature. Hydrothermal systems at active midocean ridges, for instance, expose circulating seawater to supercritical pressures and temperatures beneath the sea floor (BISCHOFF and ROSENBAUER, 1984). Separation and circulation of hydrothermal fluids in continental settings also occurs at supercritical PT conditions, as do many contact metamorphic processes. In many of these moderate- to high-temperature processes, NaCl-H_2O is the dominant fluid system (ROEDDER, 1984). In order to understand these processes occurring at supercritical conditions, knowledge of phase equilibria and critical behavior in the NaCl-H_2O fluid system is essential.

Although many workers have examined the phase behavior of NaCl-H_2O solutions, most of the critical data reported are for low salinity compositions. These show a general agreement on the location of the low-salinity segment of the NaCl-H_2O critical curve. Few studies, however, have determined critical points for fluid bulk compositions in excess of 10 wt.% NaCl and these show poor agreement. For instance, critical temperatures from critical curves plotted using the data of SOURIRAJAN and KENNEDY (1962) and URUSOVA (1974) differ by 57°C for a 20 wt.% NaCl solution. In spite of the availability of critical density data for salinities to 25 wt.% NaCl (KHAIBULLIN *et al.*, 1979), locations of the PT projections of the

critical densities (critical isochores) in the NaCl-H_2O system have not been determined in prior investigations. Furthermore, no studies to date have reported experimental critical data on NaCl-H_2O solutions with bulk compositions in excess of room temperature saturation.

The purpose of this report is to provide a consistent set of critical temperatures, pressures, densities and isochores for NaCl-H_2O solutions of up to 25 wt.% NaCl. Constraints on the critical temperatures and densities of 27.5 and 30.0 wt.% NaCl solutions are provided as well. Empirical equations fitted to experimental critical data are given as a method for estimating critical points and densities for compositions intermediate to those studied here.

PREVIOUS STUDIES

Numerous studies report experimental critical data for the NaCl-H_2O system using a variety of experimental methods (Table 1). MARSHALL and JONES (1974) determined critical temperatures of NaCl-H_2O solutions up to 9.5 wt.% NaCl by optically monitoring their behavior during heating in fused silica capillary tubes. Using an isothermal decompression technique, BISCHOFF and ROSENBAUER (1984), established that the liquid-vapor curve for standard seawater in the vicinity of the critical point is almost identical to that of 3.2 wt.% NaCl. Applying this same technique, ROSENBAUER and BISCHOFF (1987) determined critical pressures and compositions along the 450°, 475°, and 500°C isotherms. Critical temperatures, pressures, and densities for compositions from 0 to 25 wt.% NaCl were determined by KHAIBULLIN *et al.* (1979) by counting γ quanta passing through liquid and vapor phases of NaCl-H_2O solutions. Sampling liquid and vapor fluid components over a range of pressures and temperatures, SOURIRAJAN and KENNEDY (1962) determined the PTX properties, including critical points, of NaCl-H_2O solutions to 26.4 wt.% NaCl. Additionally, somewhat less extensive presentations of critical pressures and temperatures are given by URUSOVA (1974) for salinities of 9, 15, and 20 wt.% NaCl, and by ÖLANDER and LIANDER (1950) for compositions of 0.2 to 7 wt.% NaCl.

Table 1: Summary of experimentally determined critical properties in the $NaCl-H_2O$ system.

Author	Salinity Range	Data Reported
BISCHOFF and ROSENBAUER (1984)	3.2 wt.% NaCl	P, T
KHAIBULLIN *et al.* (1979)	0-25 wt.% NaCl	P, T, ρ
MARSHALL and JONES (1974)	0.6-9.5 wt.% NaCl	T
ÖLANDER and LIANDER (1950)	0.2-7 wt.% NaCl	P, T
ROSENBAUER and BISCHOFF (1987)	8.7-13.9 wt.% NaCl	P, T
SOURIRAJAN and KENNEDY (1962)	0-26.4 wt.% NaCl	P, T
THIS STUDY	0-30 wt.% NaCl	P, T, ρ

TOPOLOGY OF THE NaCl-H_2O SYSTEM

In the H_2O system, liquid, vapor, and solid (ice) coexist in equilibrium at the H_2O triple point (T; Fig. 1) which occurs at +0.01°C and 0.006 bars (HAAR *et al.*, 1984). Solid-liquid (S+L; Fig. 1), solid-vapor (S+V; Fig. 1), and liquid-vapor (L+V; Fig. 1) equilibria represent univariant reactions defined by lines in PT space (Fig. 1). The critical point at 374°C and 220 bars (HAAR *et al.*, 1984) defines the termination of the liquid-vapor curve and represents that temperature beyond which there is no longer any distinction between liquid and vapor. The critical isochore is tangent to the liquid-vapor curve at the critical point and extends from the critical point to higher PT conditions (Fig. 2).

Addition of NaCl to H_2O reduces the vapor pressure along the liquid-vapor curve and lowers the freezing point of aqueous solutions (Fig. 3). The invariant triple point of H_2O becomes a univariant melting curve in the NaCl-H_2O system along which liquid, vapor, and solid (ice) coexist in equilibrium along the join between the H_2O triple point (T(H2O); Fig. 3) and the NaCl-H_2O eutectic (E; Fig. 3). Liquid, vapor, and halite are in equilibrium along the NaCl-H_2O solubility curve (L+V+NaCl; Fig. 3), extending from the NaCl-H_2O eutectic to the NaCl triple point (T (NaCl); Fig. 3). Below this solubility curve, NaCl-H_2O vapor coexists with solid NaCl.

Two of the most important effects of added NaCl in terms of this study are (1) the extension of the critical point to higher temperatures and pressures (discussed later in detail) from the critical point of water (C(H2O); Fig. 3) to the critical point of NaCl (C(NaCl); Fig. 3) along the NaCl-H_2O critical curve (Critical Curve; Fig. 3), and (2) the appearance of a field of liquid and vapor

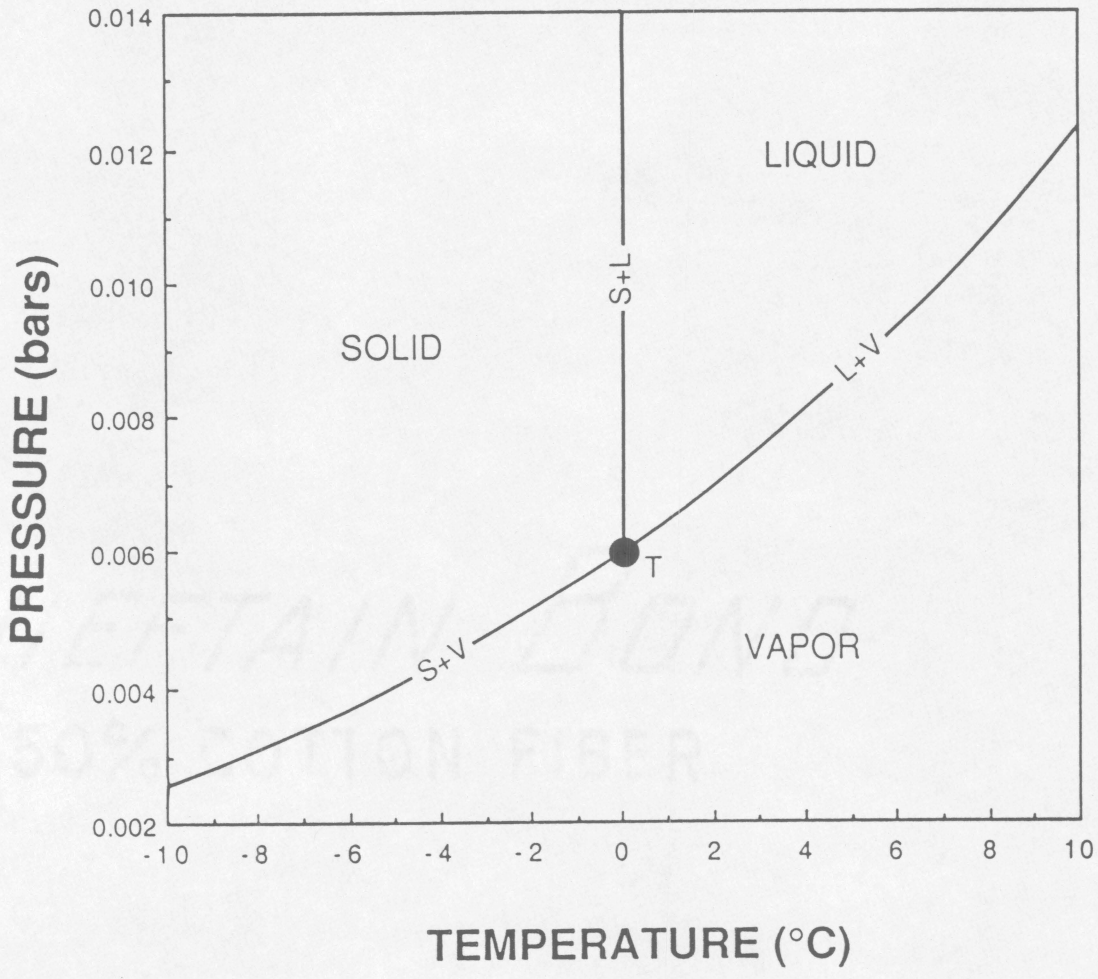

Fig. 1: Phase relations in the pure H_2O system in the vicinity of the triple point (T) at 0.01°C, 0.006 bars. Constructed from data of KEENAN *et al.* (1978) and EISENBERG and KAUZMANN (1969). Symbols explained in text.

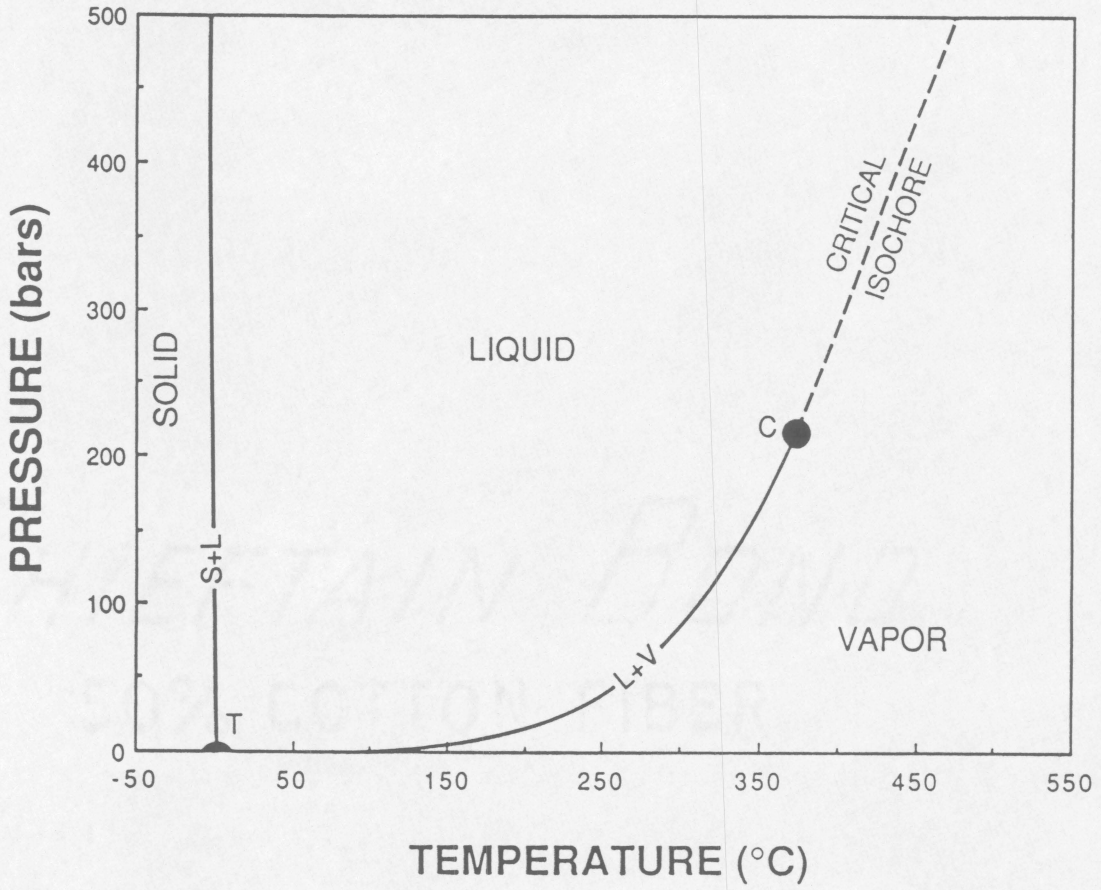

Fig. 2: Phase relations in the pure H_2O system to 500 bars and 550°C. Constructed from data of KEENAN *et al.* (1978) and HAAR *et al.* (1984). Symbols explained in text.

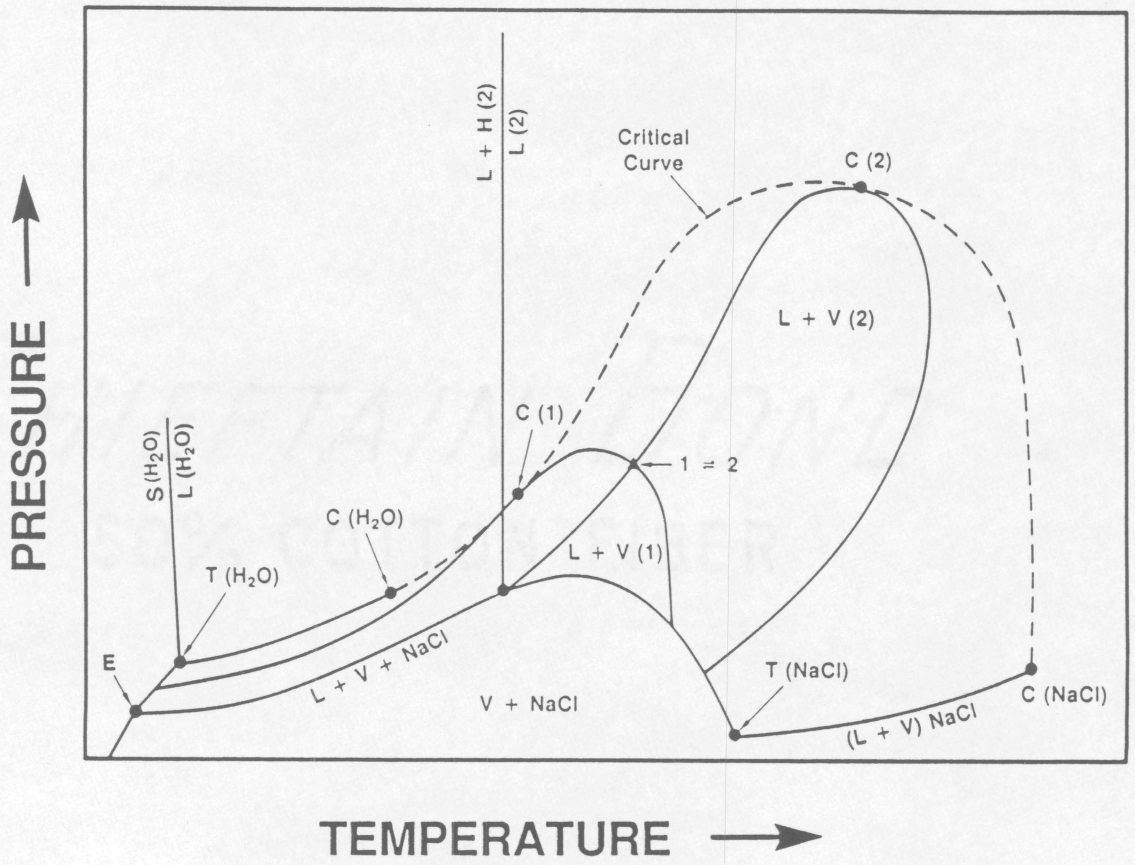

Fig. 3: Distorted schematic diagram of the topology of the NaCl-H_2O system in PT space, from Bodnar *et al.* (1985). NaCl-H_2O eutectic (E) located at 0.001 bar and -20.8°C, H_2O triple point (T) at 0.006 bar and 0.01°C, H_2O critical point (C(H2O)) at 220 bar and 374°C, NaCl critical point (C(NaCl)) at ~258 bar and ~3600°C, NaCl triple point (T(NaCl)) at ~1 bar and 801°C. Also shown are the halite liquidus ((L+H)(2)|L(2)) for a fluid of bulk composition '2', and the solid-liquid boundary (S(H_2O)|L(H2O)) for pure H_2O. Note: hydrohalite is the stable solid phase along the NaCl-H_2O solubility curve (L+V+NaCl) from the eutectic to 0.1°C. Other symbols explained in text.

immiscibility enclosed within the critical curve, liquid-vapor curves, and the solubility curves. Thus, the liquid-vapor equilibria become divariant reactions in the NaCl-H_2O system, compared to univariant reactions in the H_2O system.

In general, single phase NaCl-H_2O fluids entering this immiscibility region will separate into coexisting liquid and vapor phases. Specifically, within this region each bulk composition defines a field of immiscibility, or two-phase field, enclosed within the isoplethal liquid-vapor loop. Two such individual immiscibility fields corresponding to a low salinity fluid (composition '1') and a high salinity fluid (composition '2') are shown in figure 3. Fluids of bulk composition '1' will separate into two immiscible phases in the region labelled ((L+V)(1); Fig. 3), while fluids of bulk composition '2' will be immiscible in the region labelled ((L+V)(2); Fig. 3). Outside of their individual immiscibility fields, fluids in the NaCl-H_2O system exist as single phase liquid or vapor fluids. Within this general immiscibility field lies the single intersection of the two isopleths (1⇔2; Fig. 3). At this PT condition, any fluid of a bulk composition between that of fluids '1' and '2' will separate into two coexisting phases consisting of a low salinity vapor phase of composition 1 in equilibrium with a high salinity liquid phase of composition 2.

In the H_2O system, the liquid and vapor phase fields share the liquid-vapor curve as a common border in PT space (Fig. 2). This configuration is such that for any given temperature along this two-phase curve, liquid and vapor coexist. The high-density liquid phase field is found at pressures greater than the two-phase curve while the more compressible, low-density vapor phase is stable at lower pressures. Furthermore, the H_2O critical point serves as terminus for the H_2O liquid-vapor curve (Fig. 2).

Beyond the critical point, there exists only a single-phase, supercritical fluid. This single-phase fluid has liquid-like properties at pressures and temperatures at which its density is greater than the critical density. Correspondingly, to the high-temperature side of the critical isochore, fluid density is less than the critical density and this single-phase fluid has vapor-like properties (Fig. 2).

In the NaCl-H_2O system, liquid-vapor equilibria for a given bulk composition are represented by a field in PT space, as compared to a line in the one-component pure H_2O system. For a given composition, the liquid-vapor field (L+V; Fig. 4) is bounded at lower pressures by the L+V+NaCl curve (Fig. 4), and is bounded at lower temperatures by the ice-melting curve which extends from the eutectic point (E; Fig. 3) to the melting temperature of ice for that particular composition (Tm (ice); Fig. 4). The two phase, liquid-vapor field is separated from the single fluid phase field by a line extending from the ice-melting temperature (Tm (ice); Fig. 4) to higher temperatures and finally to its intersection with the L+V+NaCl curve (A; Fig.4). Unlike the pure H_2O system, in which the critical point represents the terminus of the liquid-vapor curve, the critical point for a given composition in the NaCl-H_2O system is a single point along the continuous liquid-vapor phase boundary that extends from the ice-melting point (Tm (ice); Fig. 4) to the three phase L+V+NaCl curve (A; Fig.4). The critical isochore begins at the critical point, tangent to the liquid-vapor boundary, and extends to higher temperatures and pressures. The critical isochore ($\rho=\rho_c$; Fig. 4) separates the one-fluid-phase field into fluids having a density greater than the critical

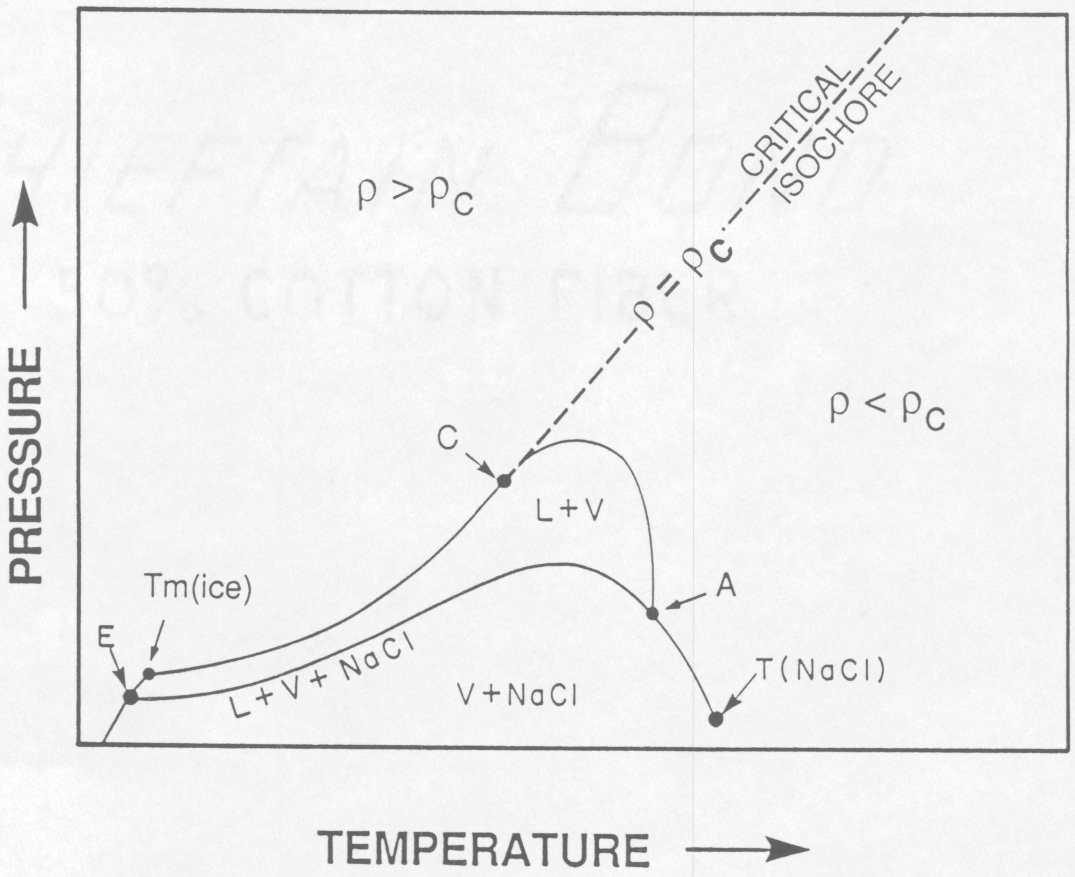

Fig. 4: Distorted schematic phase diagram of a particular NaCl-H_2O composition illustrating density relationships in the single phase region. Above the field of immiscibility (L+V), single phase NaCl-H_2O fluids are stable as liquids ($\rho>\rho c$), as vapors ($\rho<\rho c$), or as critical fluids ($\rho=\rho c$) (ρ=density; ρc=critical density). The critical point (C) is located at the point of tangency of the critical isochore with the liquid-vapor loop. Also shown are the ice-melting point (Tm (ice)) and intersection of the liquid-vapor curve with the three phase curve (A).

density ($\rho > \rho_c$; Fig. 4) and those having densities less than the critical density ($\rho < \rho_c$; Fig. 4).

The addition of NaCl to H_2O has a very dramatic effect upon critical properties. A slight addition of NaCl raises the critical temperature of an NaCl-H_2O solution. This rise in temperature in turn produces an increase in vapor pressure at the critical point. Each further addition of NaCl continues to raise the critical temperatures and pressures of NaCl-H_2O solutions, resulting in an extension of the critical curve from 374°C and 220 bars (KEENAN *et al.*, 1978) to higher pressures and temperatures.

A competing effect associated with the addition of NaCl is a decrease in the vapor pressure resulting from the dilution of H_2O with NaCl. At low to moderate NaCl concentrations, this vapor pressure reduction is more than counteracted by the effects of the increase in critical temperatures. However, with higher NaCl content, these opposing effects become equal, causing the NaCl-H_2O critical curve to reach a maximum pressure of approximately 2500 bars at 2000°C (PITZER, 1984). Further addition of NaCl continues to increase critical temperatures, but critical pressures begin to decrease rapidly from this point as the high NaCl content causes the vapor pressures to decrease. Eventually, the locus of individual critical points within the NaCl-H_2O system reaches the critical point of NaCl at ~3600°C and ~258 bars (PITZER, 1984), completing the NaCl-H_2O critical curve.

EXPERIMENTAL PROCEDURE

The experimental procedure for producing synthetic fluid inclusions is briefly summarized here and more fully described in Appendix 1. Fluid inclusions are synthesized by healing fractures in quartz in the presence of fluids of known composition at known pressures and temperatures. Synthetic fluid inclusions are obtained by placing thermally fractured inclusion-free quartz cores into platinum capsules along with dry amorphous silica powder and a few microliters of NaCl-H_2O solutions. Samples of fluids with NaCl content greater than room-temperature saturation are similarly prepared, with solid NaCl added to achieve the desired fluid bulk composition. The capsules are sealed with an arc welder and placed in cold seal pressure vessels. PT paths followed to final run conditions are chosen to avoid intersecting immiscibility fields in the NaCl-H_2O system, estimated from the data of BODNAR *et al.* (1985). Pressures are read to the nearest 5 bar interval on a factory-calibrated Heise guage traceable to NBS with an estimated accuracy of ±10 bars. Temperatures are measured and controlled to the nearest 1.0°C with chromel-alumel thermocouples and are estimated to be accurate within ±2.0°C. Run durations are typically three to seven days at conditions at 550-850°C and 1-2 kb.

Upon cooling to room temperature, runs are depressurized, and the platinum capsules are removed from pressure vessels and examined for evidence of leakage or rupture. Quartz cores, carefully removed from capsules, are cut into millimeter thick slices and polished until a smooth, glassy surface is produced. Polished samples are examined using a petrographic microscope equipped with a Fluid Inc. adapted USGS-type gas

flow heating/freezing stage. This configuration allows samples to be monitored optically over the temperature range -198°C to +700°C. Samples were frozen to verify their salinity, and approximately 6 to 10 homogenization temperatures were measured across each sample. Critical temperatures recorded have an associated accuracy of ±0.2°C at the critical point of pure water, ±2.0°C at 573°C, and an estimated ±5.0°C at 660°C, based upon prior calibration of the heating/freezing stage and observations of the α/β quartz transition.

Optimal run conditions are determined by phase equilibria of the fluid in contact with the fractured quartz. It is this dependence of the mode of homogenization of NaCl-H_2O fluid inclusions upon the trapping conditions that allows determination of critical properties using the synthetic fluid inclusion technique. For example, consider an NaCl-H_2O fluid inclusion formed along an isochore of a density greater than the critical density (as at point 1, Fig. 5). Upon heating, inclusion '1' will homogenize to the liquid phase (L+V⇒L; Fig. 5) by shrinkage and disappearance of the vapor bubble at a temperature (Th (1); Fig. 5) defined by the intersection of its isochore with the liquid-vapor curve (X; Fig. 5), a temperature less than the critical temperature for that composition. Correspondingly, a fluid inclusion with a density less than the critical density (as at point 2, Fig. 5) will homogenize by expansion of the vapor phase to fill the inclusion (L+V⇒V; Fig. 5) at a temperature (Th (2); Fig. 5) also defined by the intersection of its isochore with the liquid-vapor curve (Y; Fig. 5), which is greater than the critical temperature.

Fluids of critical density can only be trapped at the critical point

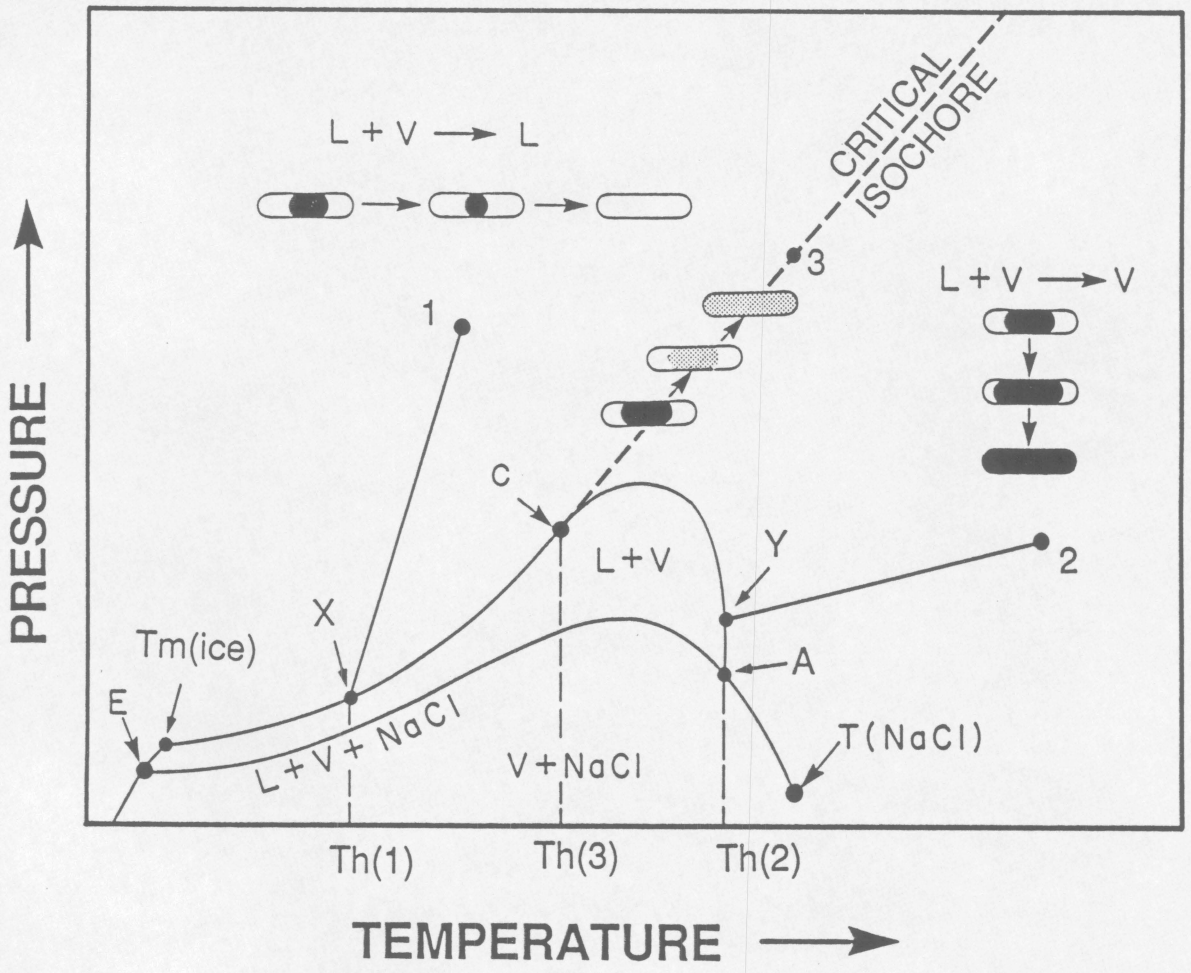

Fig. 5: Distorted schematic diagram of an NaCl-H_2O composition illustrating the relationship between homogenization behavior of NaCl-H_2O fluid inclusions and trapping conditions relative to the location of the critical isochore (see text for explanation).

(C; Fig. 5) or along the critical isochore (as at point 3, Fig. 5). These critical fluid inclusions will not homogenize by evaporation of the liquid phase or by condensation of the vapor phase. Rather, the salinity and density of the vapor will increase towards critical values as those of the liquid fall to meet them. This mutual approach of physical properties causes the meniscus separating liquid from vapor to fade gradually and finally to disappear upon homogenization at the critical temperature (Th (3); Fig. 5).

As a result of the long-range nature of the ionic forces between Na^+ and Cl^- in solution, variations in density in the vicinity of a critical point are not as large in the NaCl-H_2O system as in the H_2O system (BISCHOFF *et al.*, 1986). Still, some range in near-critical densities is expected near the binary critical isochores. Indeed, inclusions trapped adjacent to, but not on a critical isochore will frequently display near-critical behavior (ROEDDER, 1984). This behavior is manifest in the 'boiling' appearance and fading menisci of inclusions homogenizing at near-critical temperatures. Slow heating rates and careful observation of these pseudocritical inclusions reveals the true homogenization mode; menisci of inclusions of greater than critical density will fade greatly prior to shrinking, those of inclusions with less than critical density will fade as they expand.

Run conditions were chosen to bracket the critical isochore for the composition studied (Fig. 6), with some inclusions trapping a fluid with a density greater than the critical density, and others trapping a fluid of less than the critical density. Initial PT trajectories for the NaCl-H_2O system were planned on the basis of critical points reported by SOURIRAJAN and KENNEDY (1962), with isochores assumed to have positive slopes and assumed to be

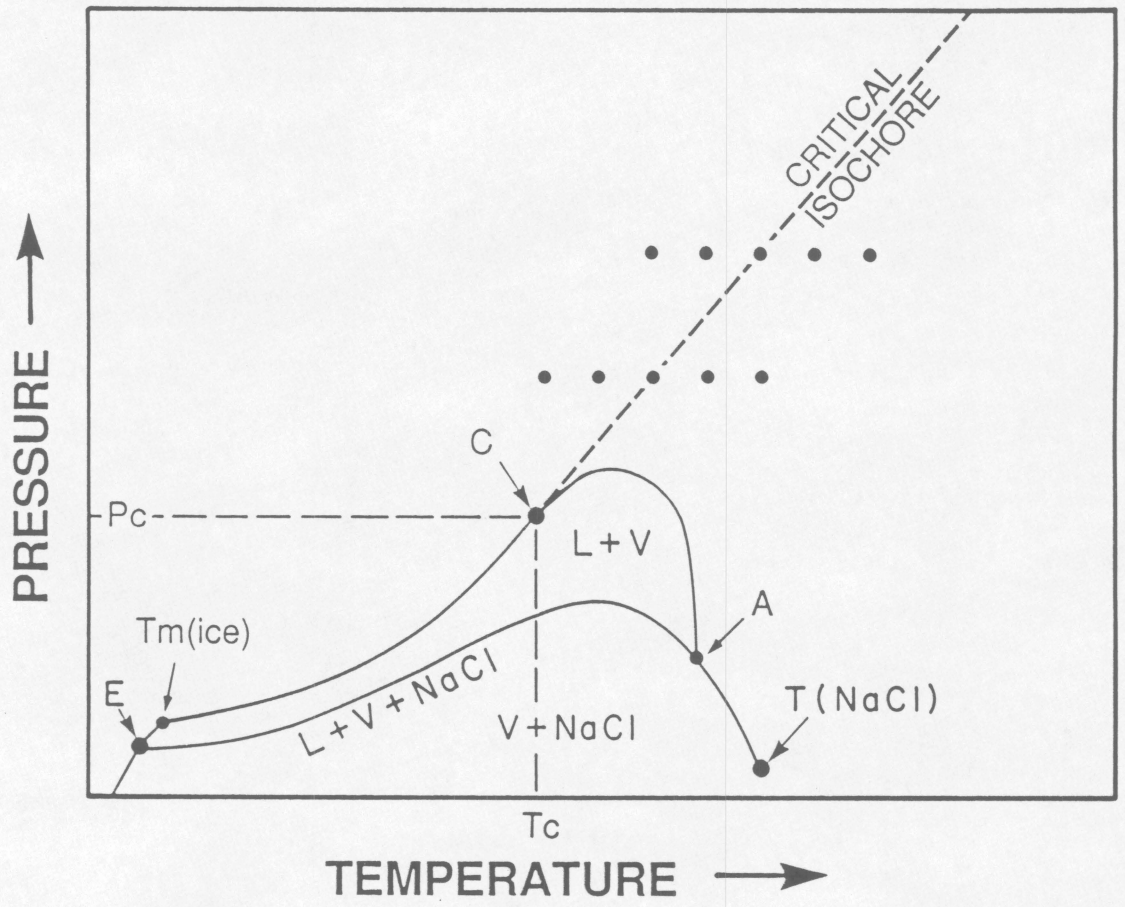

Fig. 6: Distorted schematic PT projection of the NaCl-H_2O system showing the procedure used to define the critical temperature (Tc), pressure (Pc), and isochore. Black dots represent sample run conditions. Also shown are the critical point (C), critical temperature (Tc), and critical pressure (Pc).

straight lines over relatively short ranges in pressure and temperature.

Homogenization behavior of these synthetic fluid inclusions was then used to determine the relative position of the critical isochore. Based upon this information, subsequent runs were strategically placed along these same trajectories in an iterative process until inclusions displaying critical behavior were obtained. In order to obtain confirmation of the observed critical temperatures, and to obtain the PT coordinates on a different section of each critical isochore, this entire process was repeated along a second isobaric section.

RESULTS

Critical temperatures were determined for eight different NaCl-H_2O bulk compositions, ranging from 0 to 25 wt.% NaCl. With the exception of two compositions (22.5 and 25 Wt.% NaCl), all critical temperatures were reproduced to within ±1.0°C in samples synthesized at formation conditions other than those of the initial run. Once reproducibility and precision were established, only one critical-density sample was synthesized for fluid compositions of 22.5 and 25.0 wt.% NaCl. In addition, minimum values for critical temperatures of 27.5 and 30.0 wt.% NaCl of 725°C and 682°C, respectively, were observed in samples homogenizing to the liquid phase by near-critical behavior. Critical temperatures obtained in this study are listed in Table 2 and plotted in Fig. 7. In order to predict critical temperatures for compositions intermediate to those observed, these data were regressed to produce the following empirical equation:

$$Tc = 374.1 + 8.606\,\varphi + 0.2858\,\varphi^2 - 3.189 \times 10^{-2}\,\varphi^3 + 1.013 \times 10^{-3}\,\varphi^4 \quad (1)$$

where Tc is the critical temperature in °C and "φ" is fluid composition in wt.% NaCl. Temperatures generated by equation (1) agree with measured critical temperatures in this study within ±2.5°C. As this equation was fitted to experimentally determined critical temperatures for NaCl-H_2O solutions of 0-25 wt.% NaCl, it should not be used for higher salinities.

Critical pressures for these compositions (Fig. 8, Table 2) were obtained graphically. Each critical pressure was assumed to be identical to the pressure at which the critical isochore (discussed below) intersects the

Table 2: Critical pressures, temperatures, and densities for certain compositions in the NaCl-H_2O system.

Wt.% NaCl	T(°C)	P(bars)	ρ (g/cc)
0.0	374	220	0.3220
3.2	404	298	0.4435
5.0	421	337	0.4808
10.0	466	458	0.5545
15.0	513	598	0.6112
20.0	565	755	0.6544
22.5	611	840	0.6614
25.0	665	930	0.6640
27.5	>725		<0.6782
30.0	>680		<0.7092

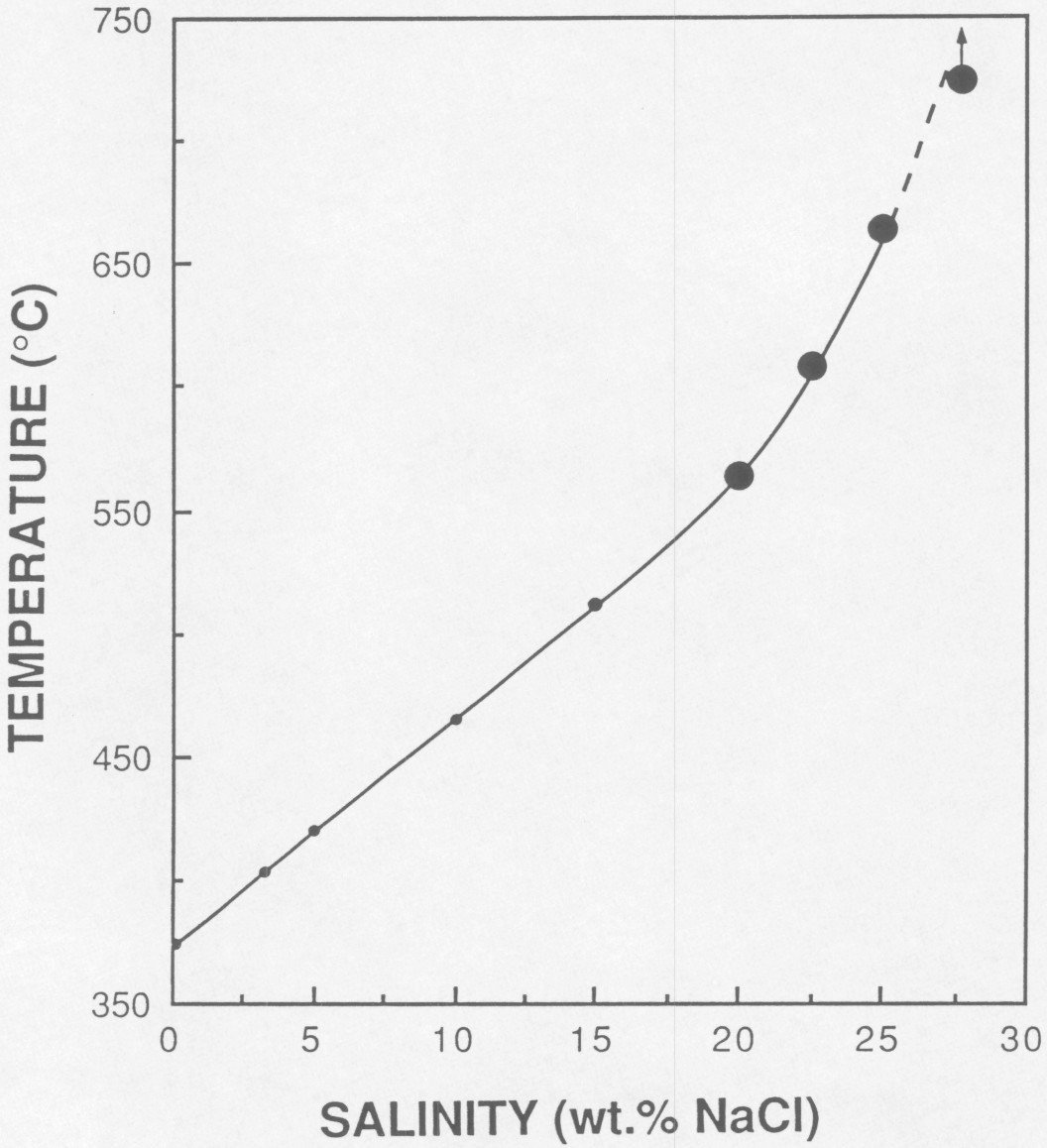

Fig. 7: Critical temperatures of NaCl-H_2O solutions determined using synthetic fluid inclusions. The line corresponds to equation (1), the filled circles to data points, scaled to show uncertainty of values at higher temperatures. Sample at 27.5 wt.% NaCl is discussed in text.

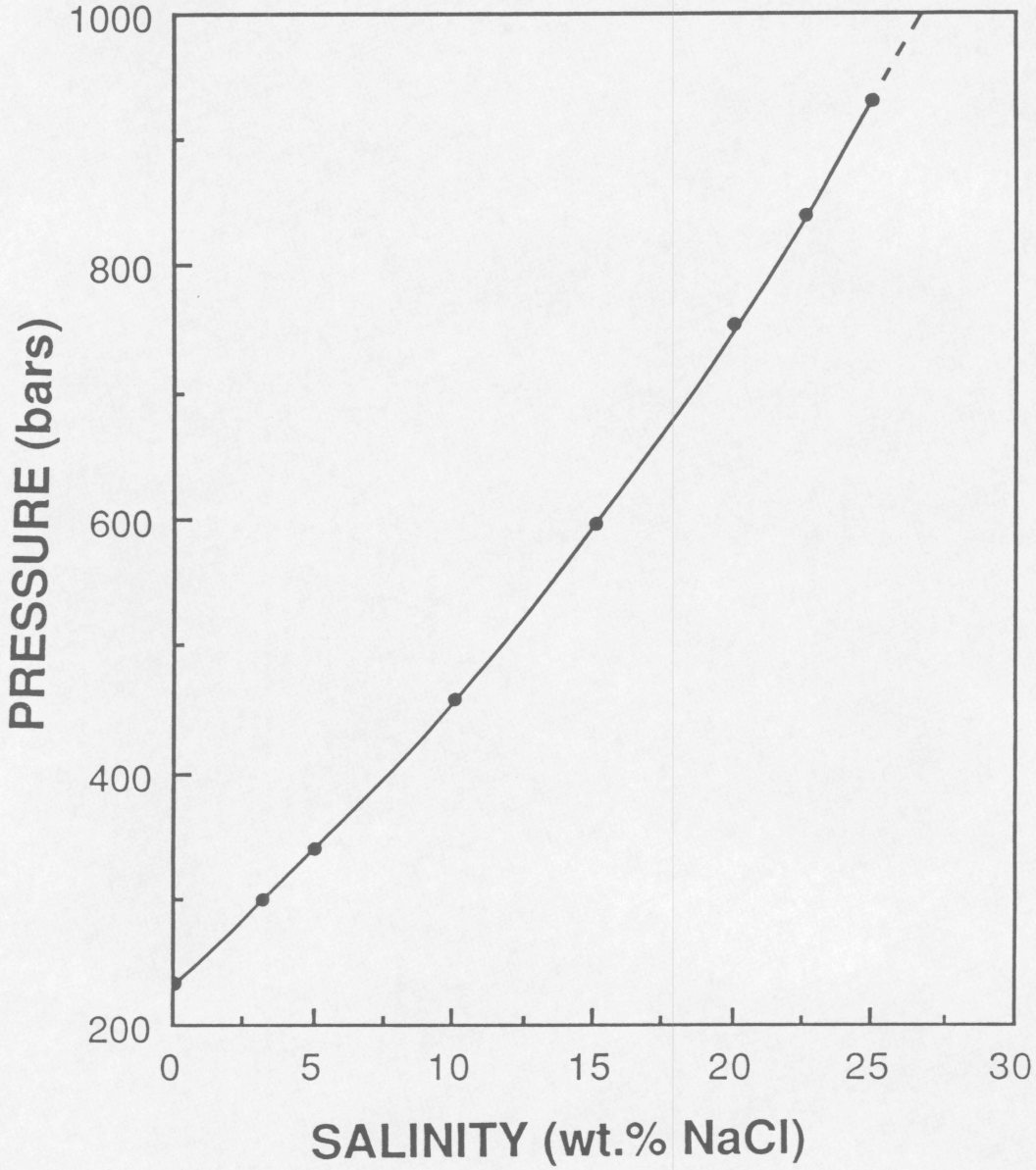

Fig. 8: Critical pressures of NaCl-H_2O solutions determined using synthetic fluid inclusions. The line corresponds to equation (2), the filled circles to pressures determined in this study.

critical temperature in PT space (Fig. 6). As the critical isochores must be extrapolated below 1000 bars from data points above this isobar (again, explained below), the accuracy of these critical pressure values is thought to be lower than that of the critical temperatures. The relationship between critical pressure and composition in the NaCl-H_2O system (to 25 wt.% NaCl) is given by equation 2:

$$Pc = 220 + 22.36\,\varphi + 9.477 \times 10^{-2}\,\varphi^2 + 5.810 \times 10^{-3}\,\varphi^3 \qquad (2)$$

where Pc is the critical pressure in bars and "φ" is composition in wt.% NaCl. Critical pressures calculated with equation (2) reproduce critical pressures determined graphically within ±3 bar. Critical pressures generated by equation (2) were combined with critical temperatures calculated using equation (1) to determine the PT trend of the NaCl-H_2O critical curve (Fig. 9).

Critical densities for all compositions studied were calculated using the equation of BODNAR (1985) relating molar volumes of NaCl-H_2O fluids to PTX properties over ranges of 100-900°C and 1-5 kb (Fig. 10, Table 2). Additionally, upper limits on critical density values are provided by the densities of the 27.5 and 30.0 wt.% NaCl samples homogenizing to the liquid phase by near-critical behavior. Critical densities calculated for samples of identical composition trapped at different formation conditions vary by less than 0.46%. For example, 10 wt.% NaCl inclusions with densities 1.34% (0.0074 g/cc) or more above or below the critical density will homogenize by non-critical behavior at temperatures other than the critical temperature. An empirical equation relating critical density to composition is given by:

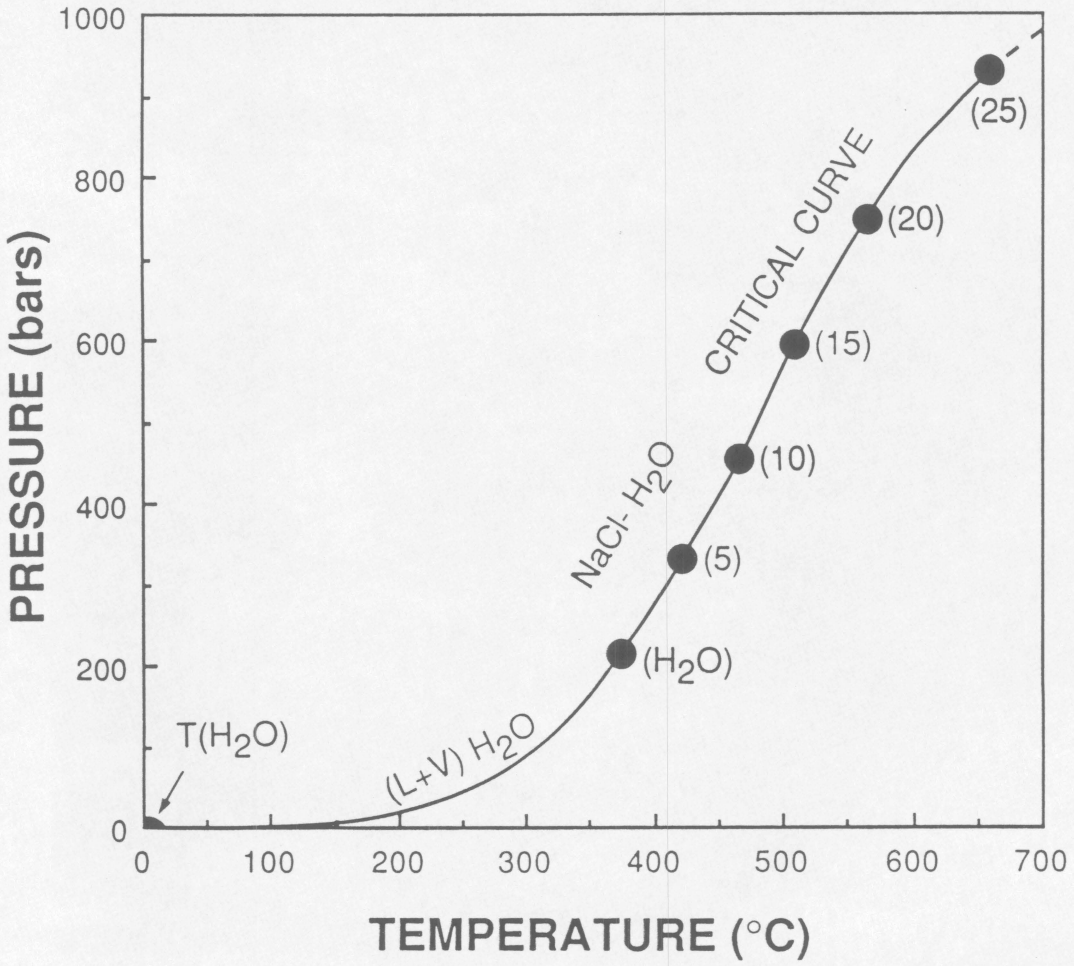

Fig. 9: NaCl-H_2O critical curve to 700°C, with compositions (wt.% NaCl) of individual critical points in parentheses. Also shown are the H_2O triple point ($T(H_2O)$) and the H_2O liquid-vapor curve ($(L+V)H_2O$) of KEENAN *et al.* (1978).

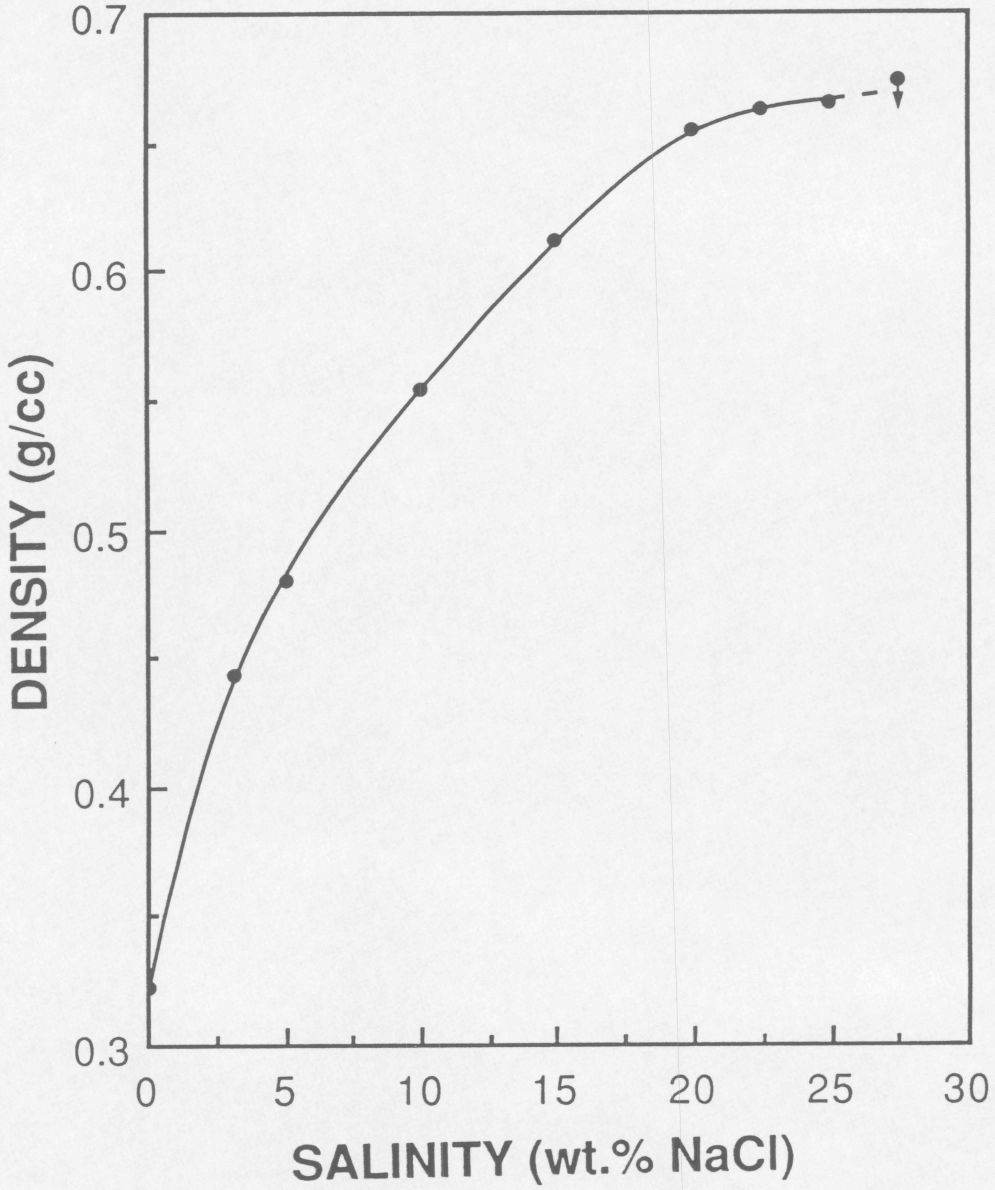

Fig. 10: Critical densities of NaCl-H_2O solutions determined using synthetic fluid inclusion data and equation of BODNAR (1985). Line corresponds to equation (3), filled circles to densities so determined. Filled circle with arrow represents density of 27.5 wt.% NaCl sample discussed in text.

$$\rho_c = 0.3220 + 5.264 \times 10^{-2}\,\varphi - 5.895 \times 10^{-3}\,\varphi^2 + 4.216 \times 10^{-4}\,\varphi^3 - 1.455 \times 10^{-5}\,\varphi^4 + 1.850 \times 10^{-7}\,\varphi^5 \qquad (3)$$

where ρ_c is the critical density (g/cc) and "φ" is composition in wt.% NaCl. Critical densities calculated with equation (3) reproduce critical densities calculated using the equation of BODNAR (1985) within ±0.25%. As predicted by the observed increase in critical density with increasing salinity, synthetic fluid inclusions of the critical density display a decrease of vapor to liquid volume ratios with increasing salinity at room temperature (Figures 11-16).

The PT projection of each critical density at temperatures below 1000°C and pressures greater than or equal to 1000 bars was calculated using the NaCl-H_2O PVTX equation of BODNAR (1985). The close proximity of immiscibility fields to critical isochores and the increased rate of variation in near-critical densities at lower pressures makes it extremely difficult to obtain experimental data in these low pressure regions. This difficulty neccessitates extrapolation of the critical isochores to pressures less than 1000 bars. Critical isochores so determined are plotted and extrapolated to lower pressures (Fig. 17). Critical isochores in the NaCl-H_2O system display an observable, slight concavity towards higher pressures. Furthermore, the degree of concavity increases with increasing salinity. As stated earlier, the critical pressures are determined in these plots at the point of intersection of the critical isochore with its own critical temperature. In all cases, these calculated critical isochores are coincident with the PT coordinates of critical isochores provided by synthetic fluid inclusions. Furthermore, synthetic

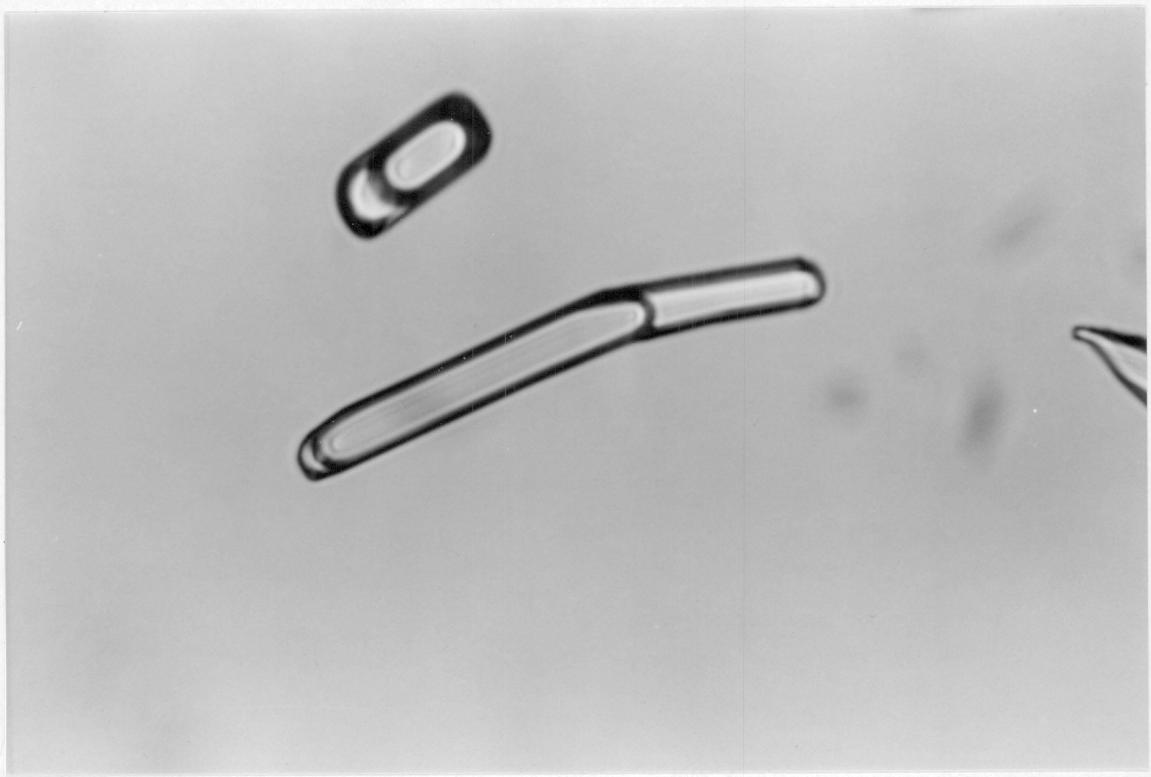

Fig. 11: Photomicrograph of H_2O synthetic fluid inclusion of the critical density at 25°C. Field of view is 160 μm in width.

Fig. 12: Photomicrograph of 5 wt.% NaCl synthetic fluid inclusion of the critical density at 25°C. Field of view is 160 μm in width.

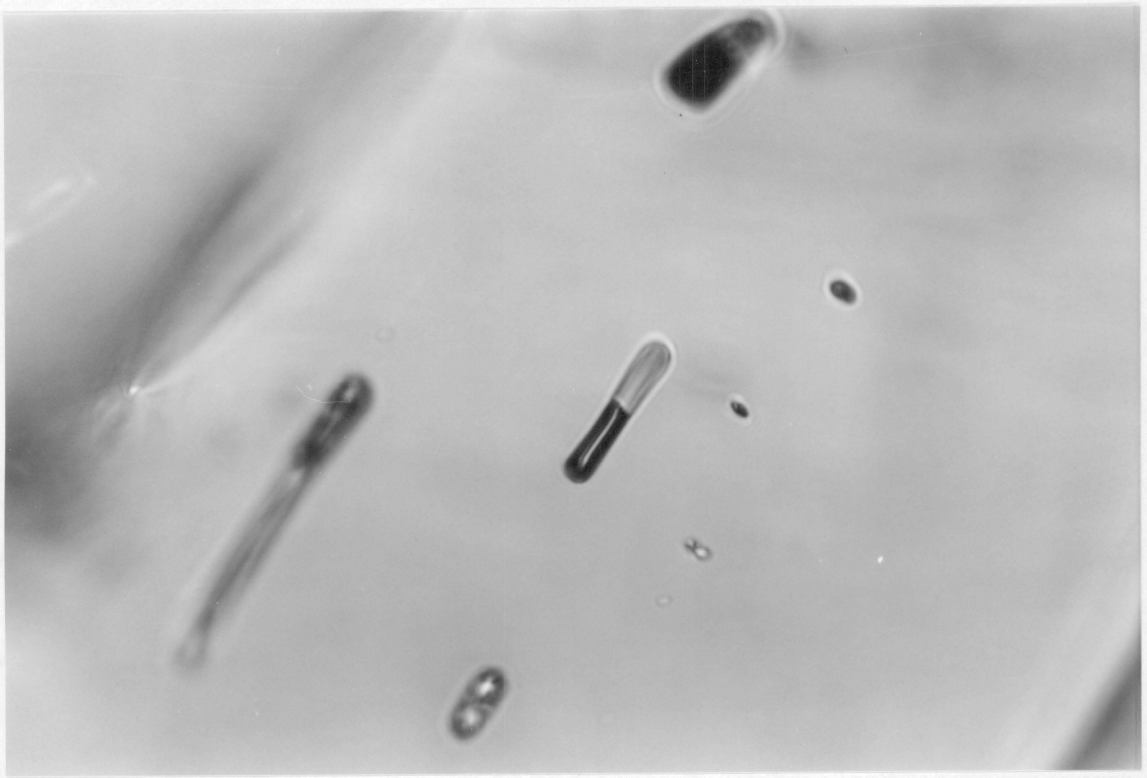

Fig. 13: Photomicrograph of 10 wt.% NaCl synthetic fluid inclusion of the critical density at 25°C. Field of view is 160 μm in width.

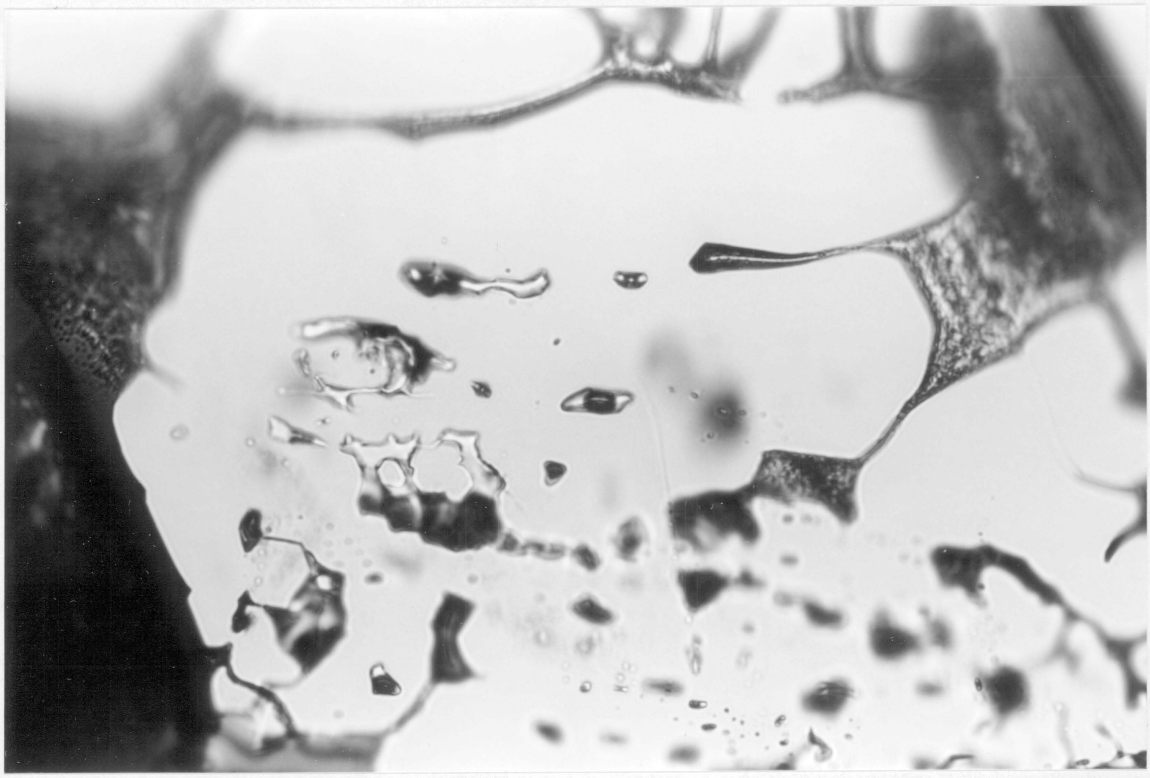

Fig. 14: Photomicrograph of 15 wt.% NaCl synthetic fluid inclusion of the critical density at 25°C. Field of view is 320 μm in width.

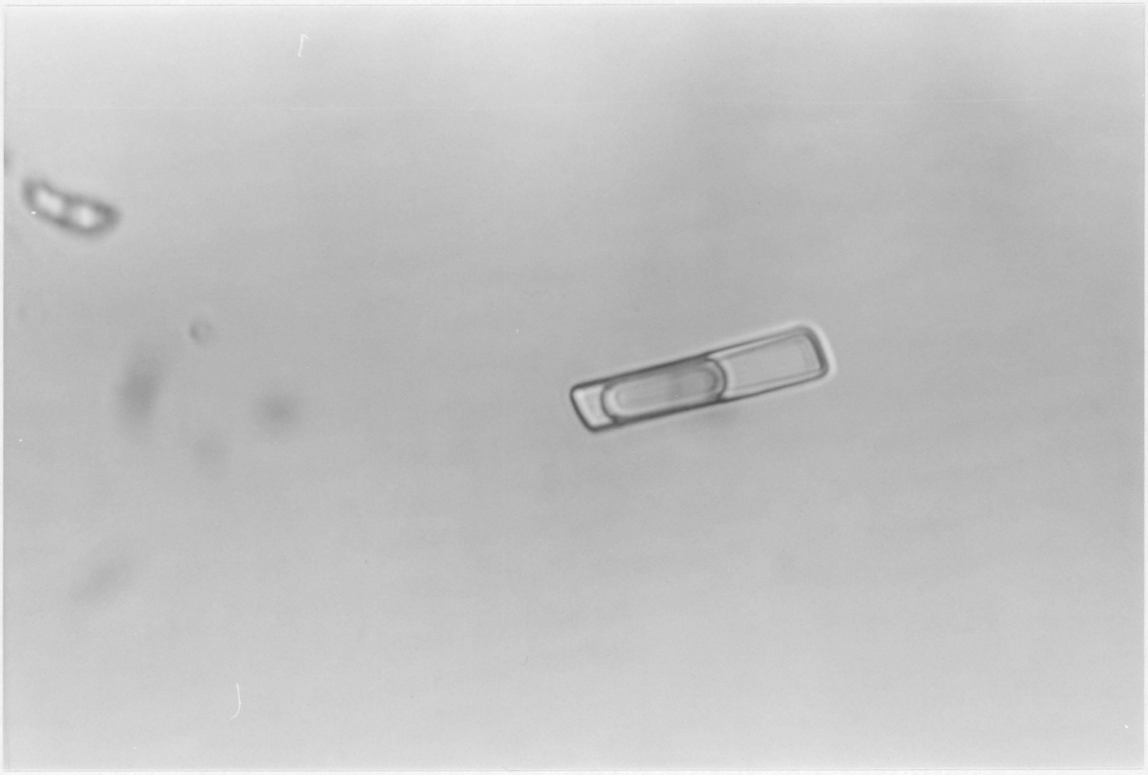

Fig. 15: Photomicrograph of 20 wt.% NaCl synthetic fluid inclusion of the critical density at 25°C. Field of view is 160 μm in width.

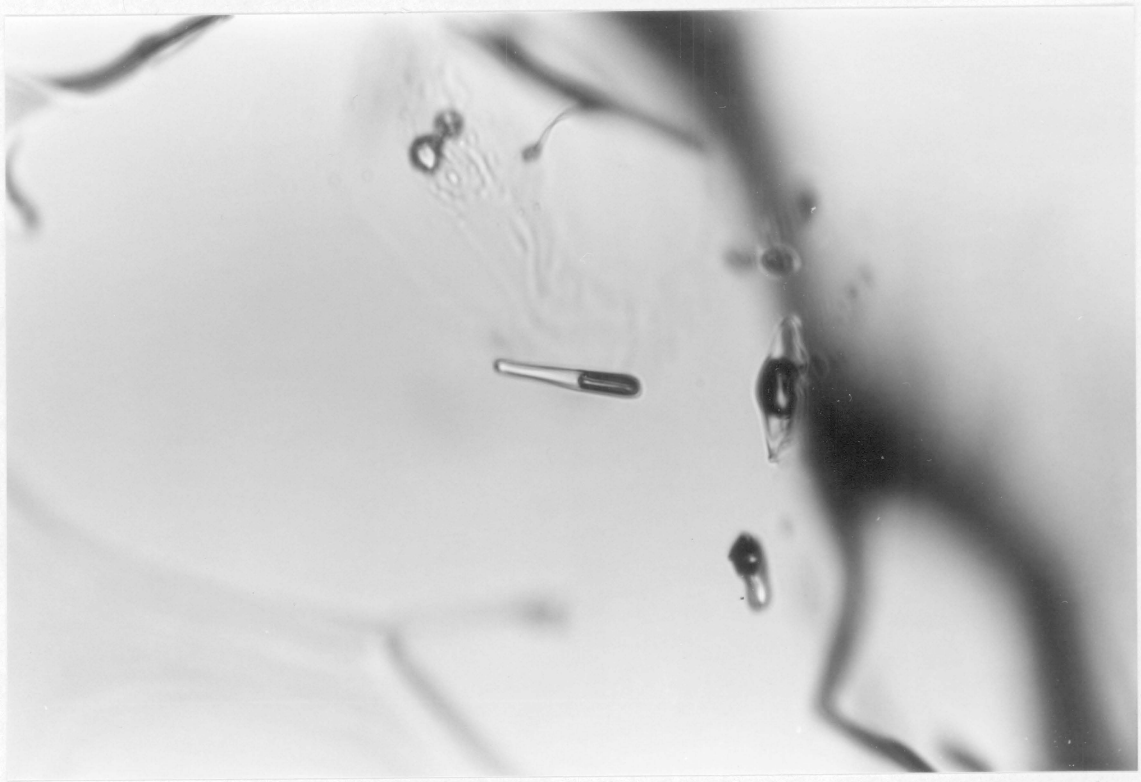

Fig. 16: Photomicrograph of 25 wt.% NaCl synthetic fluid inclusion of the critical density at 25°C. Field of view is 320 μm in width.

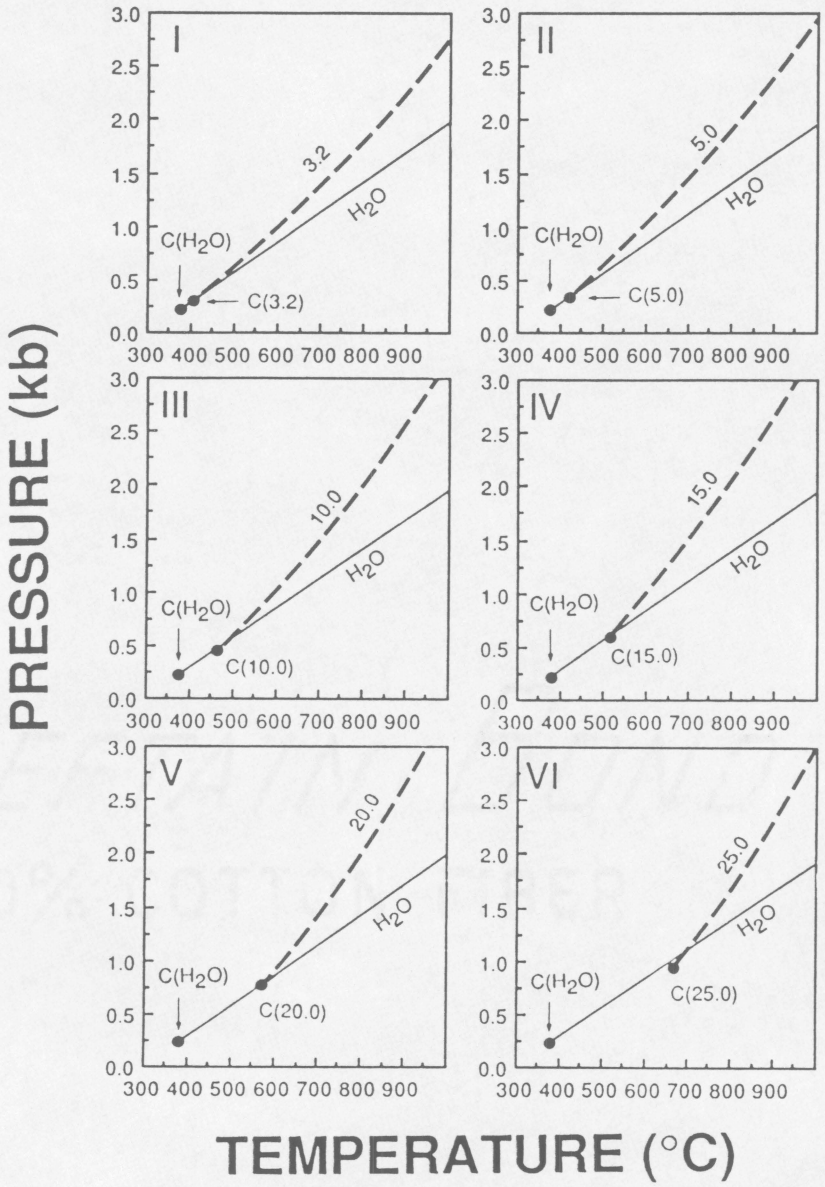

Fig. 17: Critical points (C) and critical isochores for NaCl-H_2O solutions of I) 3.2 wt.%; II) 5.0 wt.%; III) 10 wt.%; IV) 15 wt.%; V) 20 wt.%; and VI) 25 wt.% NaCl calculated from the equation of BODNAR (1985). Also shown are the critical point ($C(H_2O)$) and critical isochore (H_2O) of H_2O from HAAR *et al.* (1984). Note: NaCl-H_2O isochores are extrapolated to pressures below 1.0 kb.

inclusions which homogenize by non-critical behavior provide close brackets on all critical isochores. Inclusions trapped within ±10 bars or ±2.5°C of a critical isochore yield non-critical homogenization temperatures differing from critical by a minimum of 4°C.

COMPARISON OF RESULTS WITH PUBLISHED DATA

Critical temperatures determined in this study agree closely with previously reported experimental NaCl-H_2O critical data for salinities less than 10 wt.% NaCl (Fig. 18). At higher salinities, however, there is considerable scatter and disagreement. The critical temperatures of SOURIRAJAN and KENNEDY (1962) define the highest temperature-composition curve of all published data at these moderate salinities. The data of KHAIBULLIN *et al.* (1979) and URUSOVA (1974) predict much lower critical temperatures for a given salinity. Critical temperatures from this study are intermediate to these two, agreeing closely with the critical temperatures and compositions reported by ROSENBAUER and BISCHOFF (1987) and BISCHOFF and ROSENBAUER (1984) for compositions to ~14 wt.% NaCl.

Critical pressures reported for the NaCl-H_2O system are characterized by a common trend at salinities less than approximately 8 wt.% NaCl, present study included (Fig. 19). At greater salinities, critical pressures reported by SOURIRAJAN and KENNEDY (1962) again define a curve of higher values for common salinities than any other study. Below 25 wt.% NaCl, critical pressures of this study share a common trend with all other critical pressure reports (KHAIBULLIN *et al.* (1979), ROSENBAUER and BISCHOFF (1987), and URUSOVA (1974)).

Critical densities determined in this study are higher than those published by KHAIBULLIN *et al.* (1979) (Fig. 20). Attempts were made to evaluate this disagreement in critical density data by calculating vapor to liquid volume ratios at room temperature for critical-density fluid inclusions using a technique described by BODNAR (1983). This technique relates the

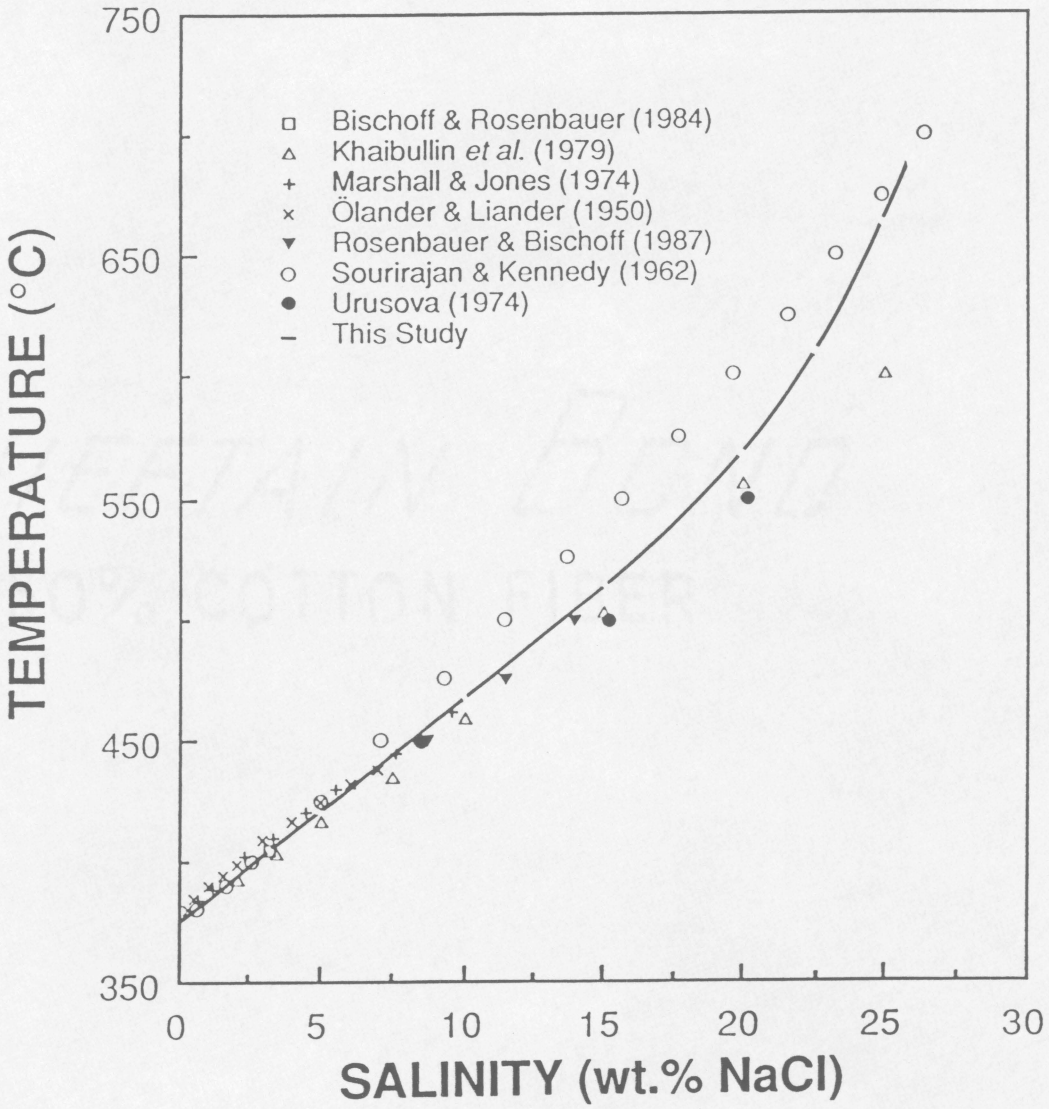

Fig. 18: Experimentally determined critical temperatures in the NaCl-H_2O system. Line corresponds to equation (1) of this study, breaks in line to position of data points.

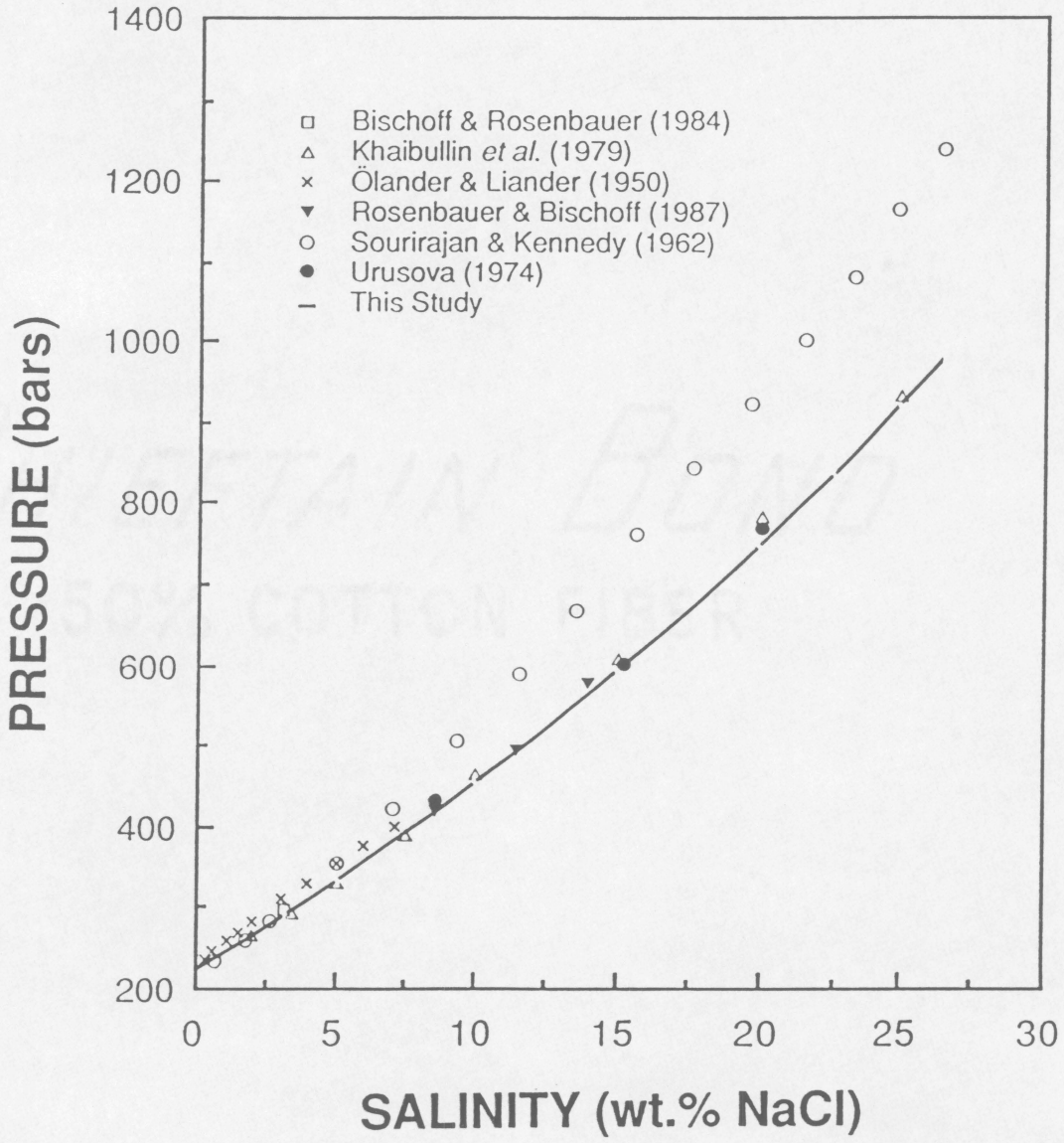

Fig. 19: Experimentally determined critical pressures in the NaCl-H_2O system. Line corresponds to equation (2) of this study, breaks in line to position of data points.

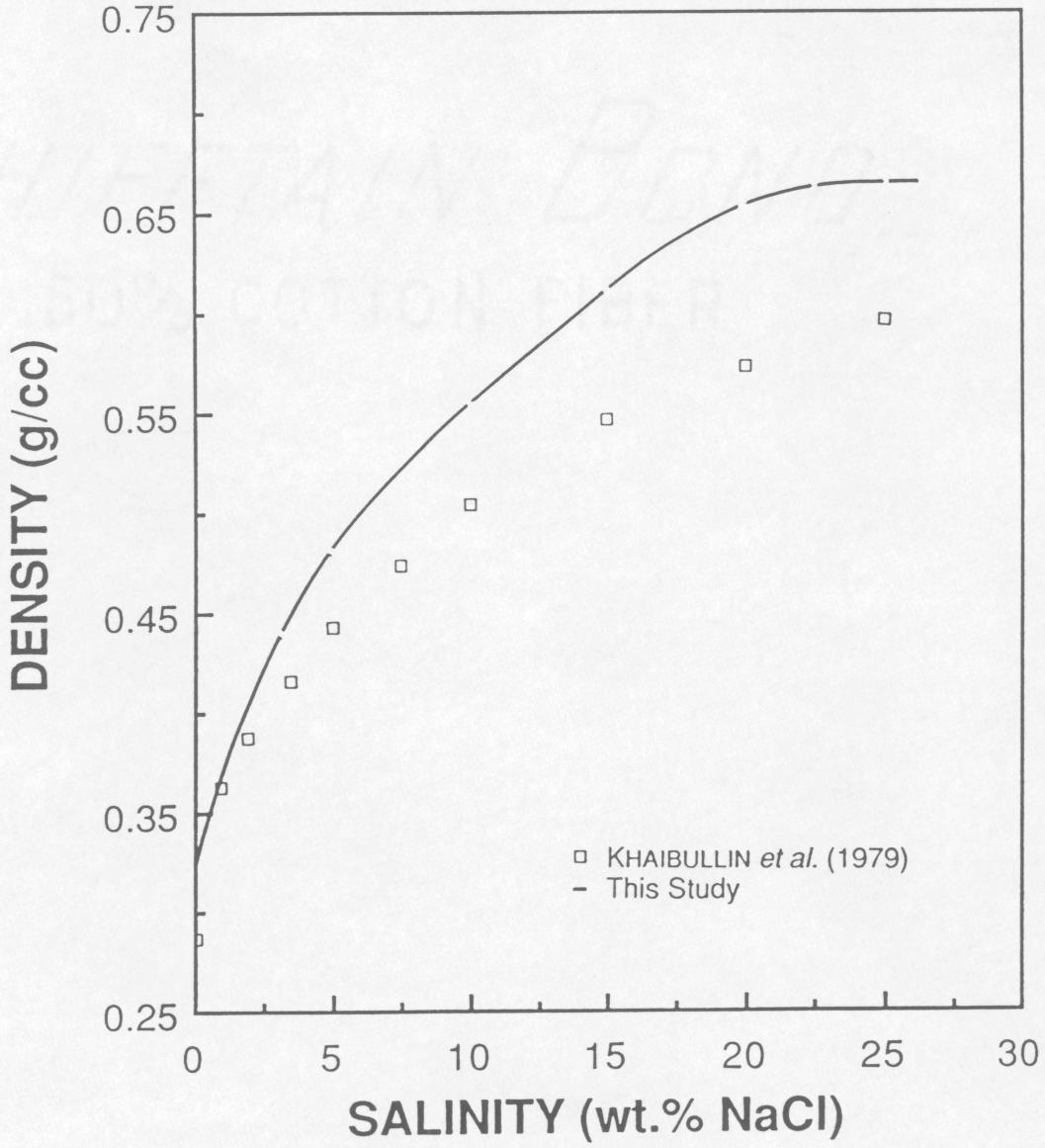

Fig. 20: Calculated critical densities in the NaCl-H_2O system. Line corresponds to equation (3) of this study, breaks in line to position of data points.

room temperature phase relations to the total inclusion density. Along with the vapor-saturated (25°C) liquid NaCl-H_2O densities of POTTER and BROWN (1977), the critical densities of KHAIBULLIN *et al.* (1979) and those of the present study were used to calculate expected volume percent vapor at room temperature for fluid inclusions homogenizing by critical behavior. Unfortunately, the critical densities of KHAIBULLIN *et al.* (1979) yield percent vapor calculations for critical fluid inclusions differing only by approximately 5% from those calculated using the critical densities of this study. Even in larger synthetic fluid inclusions, this difference is too small to distinguish accurately between the two density sets. However, the critical density of pure H_2O as reported by KHAIBULLIN *et al.* (1979) is not in agreement with other accepted published data (KEENAN *et al.* (1978) and HAAR *et al.* (1984)).

SUMMARY

Critical properties of NaCl-H_2O solutions presented in this paper represent a consistent set of critical temperatures, pressures, densities and isochores for compositions from 0 to 25 wt.% NaCl, as well as constraints on critical temperatures and densities for two salinities in excess of room temperature saturation. Critical points to 25 wt.% NaCl span a range of temperatures and pressures from 374° to 665°C and 220 to 930 bars. These values are in general agreement with a majority of previously reported critical points in the NaCl-H_2O system below approximately 20 wt.% NaCl. At higher salinities, there is no agreement as to the PT trend of the NaCl-H_2O critical curve.

REFERENCES

BISCHOFF J. L. and ROSENBAUER R. J. (1984) The critical point and two phase boundary of sea water, 200-500°C. *Earth and Planet. Sci. Letters* **68**, 172-180.

BISCHOFF J. L., ROSENBAUER R. J. and PITZER K. S. (1986) The system NaCl-H_2O: Relations of vapor-liquid near the critical temperature of water and of vapor-liquid-halite from 300° to 500°C. *Geochim. et Cosmochim. Acta* **50**, 1437-1444.

BODNAR R. J. (1983) A method of calculating fluid inclusion volumes based on vapor bubble diameters and P-V-T-X properties of inclusion fluids. *Econ. Geol.* **78**, 535-542.

BODNAR R. J. (1985) Pressure-volume-temperature-composition (PVTX) properties of the system H_2O-NaCl at elevated temperatures and pressures, Ph.D. dissert., Penn. State Univ.

BODNAR R. J., BURNHAM C. W. and STERNER S. M. (1985) Synthetic fluid inclusions in natural quartz III. Determination of phase equilibrium properties in the system H_2O-NaCl to 1000°C and 1500 bars. *Geochim. et Cosmochim. Acta* **49**, 1861-1873.

BODNAR R. J. and STERNER S. M. (1985) Synthetic fluid inclusions in natural quartz II. Applications to PVT studies. *Geochim. et Cosmochim. Acta* **49**, 1855-1859.

EISENBERG D. and KAUZMAN W. (1969) *The Structure and Properties of Water*, 296 p., New York, Oxford University Press.

HAAR L., GALLAGHER J. S. and KELL G. S. (1984) *NBS / NRC Steam Tables*, 320 p., Washington, Hemisphere.

KEENAN J. H., KEYES F. G., HILL P. G., MOORE J. G. (1978) *Steam Tables Thermodynamic Properties of Water Including Vapor, Liquid, and Solid Phases*, 156 p., New York, Wiley-Interscience.

KHAIBULLIN I. KH., NOVIKOV B. YE., COPELIOVICH A. M. and BESEDIN A. M. (1979) Phase diagrams for steam solutions and caloric properties of two- and three- component systems: H_2O-NaCl, H_2O-Na_2SO_4 and H_2O-NaCl-Na_2SO_4. In *Water and Steam*, (eds. J. STRAUB and K. SCHEFFLER), 641-647, New York, Pergammon.

MARSHALL W. L. and JONES E. V. (1974) Liquid-vapor critical temperatures of aqueous electrolyte solutions. *J. Inorganic Nuclear Chem.* **36**, 2313-2318.

ÖLANDER A. and LIANDER H. (1950) The phase diagram of sodium chloride and steam above the critical point. *Acta Chim. Scand.* **4**, 1437-1445.

PITZER K. S. (1984) Critical point and vapor pressure of ionic fluids including NaCl and KCl. *Chem. Phys. Letters* **105**, 484-489.

POTTER R. W. II and BROWN D. L. (1977) The volumetric properties of aqueous sodium chloride solutions from 0° to 500°C at pressures up to 2000 bars based on a regression of available data in the literature. *U. S. Geol. Survey Bull. 1421-C*, 36 p.

ROEDDER E. (1984) *Fluid Inclusions*, Mineral. Soc. Amer., Reviews in Mineralogy **12**, 644 p.

ROSENBAUER R. J. and BISCHOFF J. L. (1987) Pressure-composition relations for coexisting gases and liquids and the critical points in the system NaCl-H_2O at 450, 475, and 500°C. *Geochim. et Cosmochim. Acta* **51**, 2349-2354.

SOURIRAJAN S. and KENNEDY G. C. (1962) The system H_2O-NaCl at elevated temperatures and pressures. *Amer. Jour. Sci.* **260**, 115-141.

URUSOVA M. A. (1974) Phase equilibria in the sodium hydroxide-water and sodium chloride-water systems at 350-550°C. *Russian J. Inorganic Chem.* **19**, 450-454.

APPENDIX 1: EXPERIMENTAL PROCEDURES

Slabs of Brazilian quartz are cored using a diamond-studded coring bit with an inner diameter of ~4 mm. Once cleaned, these cores are thermally fractured by heating to 350-400 °C and immersing in room temperature doubly-distilled water. The fractured cores are dried overnight in an oven at approximately 150 °C to remove water from the fractures.

Platinum capsules are assembled from platinum tubing with an inner diameter of 4 mm. Cylinders approximately 20 mm in length are cut to form the capsule walls, while longer lengths are cut for use as end caps. These platinum tubes are annealed by immersion in cool distilled water after being held in a flame until cherry-red. The longer tubes are cut open, flattened, and punched with an ordinary paper punch. The platinum rounds are then shaped much like bottle caps using a specially designed tool, allowing two caps per cylinder. After cleaning caps and tubes with alcohol, one of these end caps is pushed into an open end of the cylinder and arc welded, using distilled water as a coolant and taking care to achieve a smooth, continuous weld. Both the open capsules and the remaining end cap are then cleaned with alcohol, rinsed twice in distilled water (once ultrasonically) and dried in an oven to insure evaporation of all water.

Capsules are initially loaded with small amounts of ball-milled silica to provide silica for fracture healing. Fluids are then loaded into the capsules using a 50 microliter syringe for fluids which are undersaturated with NaCl at room temperature. NaCl is added in solid form to achieve desired bulk composition for salinities in excess of 26.4 wt.% NaCl. Following addition of the fluid, fractured quartz cores are added to the capsules. The second end

cap is inserted and arc welded into place with careful application of distilled water coolant to a cotton fiber coolant jacket (a kimwipe or similar tissue). It is of great importance that the loading and sealing of capsules be accomplished with some speed and with adequate cooling in order to eliminate the effects of evaporation (and thus a change of fluid bulk composition) from the capsule. Once loaded and sealed, capsules are marked with a scribe and weighed.

Once weighed, capsules are loaded into pressure vessels, all information pertinent to them being noted in the log book. Small amounts of water are added to each bomb prior to insertion of filler rods to assist in speedy pressurization and uniform heating of the sample chamber. The bombs are shut tightly, stood upright to assure that samples are situated as far into the vessels as possible, and fitted to the pressure system.

If, during the course of the run, the sample is even briefly exposed to PT conditions within its immiscibility field, the fluid contained will separate into two phases. As the amount of fluid sealed into each capsule is quite small (on the order of a few tens of microliters), entrapment of any fluid of a salinity other than the original bulk composition will result in a change of the bulk salinity of fluids available to form new inclusions should the sample reenter a single-phase domain. Therefore, samples are taken to run conditions along PT paths chosen to avoid locations of immiscibility fields in the NaCl-H_2O system estimated from the data of BODNAR *et al.* (1985). This is accomplished by pressurizing the sample chambers prior to heating, and by further overpressuring the bombs as the temperature within the sample chamber approaches run conditions. Upon stabilization of temperature, usually accomplished within one to two hours, pressure is bled from the system until

desired run conditions are met. Pressures are read and assumed accurate to the nearest 5 bar interval on a factory-calibrated Heise guage traceable to NBS. Not only does this initial overpressuring keep the samples from entering the field of immiscibility (and so avoiding locallized changes in bulk fluid composition), it also encourages reequilibration to run conditions of any fluid inclusions formed prior to stabilization (BODNAR and STERNER, 1985).

The ovens are then pulled into position around each bomb and allowed to heat the samples. When all samples are within a temperature range of 250 to 350 °C, ductility of the platinum capsules and fluid pressure within the capsules is sufficient for the sample to survive application of higher pressures, and pressure is increased to the desired run conditions. As temperatures continue to rise within the sample chambers, a corresponding increase in pressure will occur. Runs are usually stabilized within one to two hours, and any excess pressure can be bled from the system at this time. Any inclusions formed prior to run equilibration (thus at a higher pressure than run conditions) are likely to reequilibrate to the lower pressure run conditions (BODNAR and STERNER, 1985). Given the positive slopes of isochores in the NaCl-H_2O system, any inclusions formed at higher pressures that do not reequilibrate will have higher densities (and so lower homogenization temperatures) than the bulk of the inclusions, and can be easily distinguished from the inclusions of interest. Runs are left up for a period of five to seven days, during which time temperatures and pressures are held constant and are monitored for any changes.

Taking down a run is ideally done under isobaric conditions. Lacking equipment to accomplish this, these runs are simply removed from the ovens

and left to cool, open to the common pressure line and ballast tank. Although there is some danger of entering a field of immiscibility with this technique, especially in systems where very little is known about the locations of such regions, it has presented no difficulty in the NaCl-H_2O system.

Upon cooling to room temperature, runs are depressurized, and sample recovery and processing begins. Capsules removed from pressure vessels are cleaned, reweighed, and examined microscopically for evidence of leakage or rupture. Quartz cores are removed from capsules with the aid of a pair of wirecutters (to snip off the capsule end) and a pair of needlenosed pliers (to peel the pliant platinum down and around in a spiral). Care must be taken to avoid crushing the quartz cores in this process. The cores are then rinsed and placed in pyrex tubes containing Crystalbond (thermoplastic polymer resin) and set in a warm oven until the cores have settled into the resin. After slow cooling to room temperature, the samples are cut into millimeter thick slices (called chips) using a slow speed saw and a good diamond-bearing blade. The chips are soaked for approximately ten minutes in acetone to dissolve the resin, and polished using 60 and 0.3 micron polishing powders until a smooth, glassy surface is produced.

Polished chips were examined using a Leitz petrographic microscope and a Fluid Inc. USGS-type gas flow heating and freezing stage calibrated with synthetic fluid inclusions. This configuration allows samples to be monitored optically while applying and measuring temperatures of -198°C to +700°C at the sample surface. Samples were frozen to verify their salinity, and approximately 6 to 10 homogenization temperatures were measured across each sample. Temperatures recorded are assumed accurate to ±2°C

based upon calibration of the H/F stage, the reproducibility of the critical temperatures obtained from different samples, and the low range in homogenization temperatures observed in all critical fluid inclusions.

APPENDIX 2: SYNTHETIC FLUID INCLUSION DATA

Th = Temperature of homogenization

Mode = Homogenization mode:

L = Homogenization to liquid phase

Lc = Near-critical homogenization to liquid phase

C = Homogenization by critical behavior

Vc = Near-critical homogenization to vapor phase

V = Homogenization to vapor phase

Tf = Temperature at formation, or trapping

Pf = Pressure at formation

Wt. %	Sample No.	Th(°C)	Mode	Pf(bars)	Tf(°C)	Th Range (°C)	Count
3.20	090187.09	383	L	1085	611	381.8-384.8	5
3.20	090187.10	403	L	1085	616	403.3-404.5	7
3.20	090187.11	404	Lc	1085	618	401.9-404.8	5
3.20	090187.12	405	C	1085	620.5	404.6-405.0	4
3.20	091087.01	404	C	1395	701	403.8-404.8	3
3.20	091087.03	409	Vc	1395	709	406.7-410.7	6
3.20	091087.05	411	Vc	1395	718	409.2-411.2	4
5.00	022487.01	395	L	1150	555	394.3-395.9	4
5.00	032387.01	400	L	1005	550	398.2-401.2	8
5.00	041487.01	407	L	1035	580	405.7-407.2	3
5.00	032387.03	409	L	1025	570	408.8-409.8	5
5.00	041487.03	416	Lc	1050	590	415.4-416.3	9

Wt. %	Sample No.	Th(°C)	Mode	Pf(bars)	Tf(°C)	Th Range (°C)	Count
5.00	051987.01	421	C	1000	591	420.5-421.9	8
5.00	051987.02	424	Vc	1000	600	422.7-424.8	8
5.00	032387.06	434	V	1025	599	433.4-433.7	3
5.00	031287.01	391	L	1335	598	390.4-391.6	5
5.00	031287.03	401	L	1380	625	399.4-402.1	12
5.00	022487.12	412	L	1320	649	411.6-412.2	7
5.00	041487.06	414	Lc	1355	660	413.6-414.2	2
5.00	041487.07	421	C	1315	670	419.9-421.8	11
5.00	051987.03	426	Vc	1300	675	424.4-426.0	8
10.00	022487.05	431	L	1095	564	430.2-431.4	4
10.00	032387.07	448	L	1025	585	446.8-448.7	10
10.00	022487.08	459	Lc	1055	598	458.2-460.1	9
10.00	032387.08	467	C	1025	599	466.0-468.1	3
10.00	032387.10	497	V	1055	615	491.1-505.1	5
10.00	031287.05	451	L	1320	649	450.8-452.6	6
10.00	022487.13	466	C	1375	675	465.7-466.8	5
10.00	031287.04	464	L	1380	625	463.1-466.0	9
10.00	051987.04	475	Vc	1300	675	473.7-475.3	10
15.00	022487.10	487	L	1055	598	486.6-486.8	2
15.00	022487.14	499	L	1065	609	497.2-501.7	10
15.00	041487.09	521	Vc	1050	618	520.1-526.6	6
15.00	041487.11	531	Vc	1085	624	526.5-533.3	13
15.00	090187.01	493	Lc	1060	611	492.6-494.2	2
15.00	090187.02	504	Lc	1060	616	502.7-506.1	6

Wt. %	Sample No.	Th(°C)	Mode	Pf(bars)	Tf(°C)	Th Range (°C)	Count
15.00	090187.03	509	Lc	1060	618	506.2-513.1	8
15.00	090187.04	513	C	1060	620.5	512.9-514.1	5
15.00	072087.13	491	L	1205	640	488.8-493.9	7
15.00	082687.01	498	Lc	1200	642.5	497.7-498.6	2
15.00	082687.02	514	C	1200	645	514.1-514.6	4
15.00	072087.17	503	Lc	1205	660	500.6-506.8	9
15.00	072087.19	549	V	1205	665	544.5-555.3	4
15.00	051987.05	510	Lc	1300	667	506.5-511.5	8
15.00	031287.06	512	Lc	1375	675	510.3-514.0	8
15.00	031287.07	550	Vc	1305	700	548.7-553.1	6
20.00	051287.01	503	L	1200	630	501.0-508.3	5
20.00	051287.05	538	Lc	1200	650	535.2-543.6	8
20.00	051287.07	563	Lc	1200	660	561.7-564.7	2
20.00	072087.20	566	C	1205	665	564.1-567.7	4
20.00	072087.20	569	Vc	1205	665	567.6-570.9	5
20.00	051287.09	592	Vc	1200	670	588.8-595.3	9
20.00	051287.11	629	Vc	1200	680	627.7-630.0	9
20.00	072087.21	674	V	1205	690	672.1-675.9	8
20.00	072087.01	546	Lc	1400	689	543.4-547.4	8
20.00	072087.03	565	C	1400	701	563.4-568.0	7
20.00	072087.05	599	V	1400	714	596.1-603.0	4
22.50	112487.05	582	Lc	1740	763	580.6-582.6	5
22.50	112487.06	611	C	1740	784	610.4-612.3	4
22.50	112487.07	653	Vc	1740	803	650.1-656.4	4

Wt. %	Sample No.	Th(°C)	Mode	Pf(bars)	Tf(°C)	Th Range (°C)	Count
25.00	051287.02	517	L	1200	630	512.2-519.0	8
25.00	051287.04	549	L	1200	640	545.1-550.7	8
25.00	051287.06	556	L	1200	650	551.2-557.7	8
25.00	051287.08	582	L	1200	660	579.1-584.0	7
25.00	051287.10	612	Lc	1200	670	608.4-613.9	9
25.00	051287.12	625	Lc	1200	680	620.3-630.1	8
25.00	082687.04	653	Lc	1200	685	652.2-654.7	4
25.00	082687.06	674	Vc	1200	690	671.5-675.9	5
25.00	072087.02	557	L	1400	689	556.2-557.6	4
25.00	072087.04	599	L	1400	701	596.5-602.1	8
25.00	072087.06	600	Lc	1400	714	597.0-603.0	8
25.00	091087.06	624	Lc	1395	718	622.1-625.4	6
25.00	091087.08	643	Lc	1395	720	641.9-644.6	7
25.00	091087.10	642	Lc	1395	723	641.1-643.7	6
25.00	072087.07	665	Vc	1400	725	661.2-668.0	6
25.00	072087.09	669	Vc	1400	734	665.3-675.8	7
25.00	100687.02	573	L	1965	790	572.1-573.4	6
25.00	100687.03	591	L	1965	800	590.0-590.8	4
25.00	100687.04	601	Lc	1965	813	599.1-602.2	6
25.00	100687.05	606	Lc	1965	822	602.2-611.2	3
25.00	100687.06	630	Lc	1965	834	628.7-631.6	4
25.00	110687.01	655	Lc	1960	848	654.8-655.2	4
25.00	110687.02	665	Lc	1960	845	661.3-668.2	8
25.00	110687.03	668	C	1960	852	666.9-669.9	6

Wt. %	Sample No.	Th(°C)	Mode	Pf(bars)	Tf(°C)	Th Range (°C)	Count
27.5	112487.08	670	Lc	1740	803	676.2-678.8	8
27.5	112487.09	725	Lc	1740	827	725.1	4
30.0	100687.07	593	L	1965	781	592.8-594.0	7
30.0	100687.08	603	L	1965	790	601.6-604.4	7
30.0	100687.09	612	L	1965	800	610.9-613.6	7
30.0	100687.10	628	Lc	1965	813	626.4-628.7	6
30.0	100687.11	644	Lc	1965	822	641.2-645.4	7
30.0	100687.12	656	Lc	1965	834	653.9-658.1	7
30.0	110687.04	679	L	1960	848	676.1-679.6	8
30.0	110687.05	682	L	1960	845	681.4-683.1	7
30.0	110687.06	682	Lc	1960	852	679.5-683.0	8

The vita has been removed from the scanned document